



Maximum tolerance for water content at various stages of a natuna production

Bjørn Kvamme¹ · Solomon Aforkoghene Aromada¹ · Tatiana Kuznetsova¹  · Petter Berge Gjerstad¹ · Pablo Charles Canonge¹ · Mojdeh Zarifi¹

Received: 12 March 2018 / Accepted: 24 September 2018 / Published online: 3 October 2018
© Springer-Verlag GmbH Germany, part of Springer Nature 2018

Abstract

Though the Natuna field in offshore Indonesia contains natural gas resources, its CO₂ content exceeds 70%. While existing technologies can handle the separation challenges, the question of CO₂ transport and storage will still remain due to the lack of aquifer storage sites with sufficient sealing integrity in this part of South Asia. Substantial occurrences of natural gas hydrates have been discovered in offshore Indonesia roughly 700 miles from Natuna, making the pipeline transport economically feasible. This work aimed to assess the risk of hydrate formation during this transport as evaluated by two different approaches: traditional method based on water dew-point versus evaluation accounting for alternative routes of hydrate formation. The hydrate risk analysis was also conducted for produced natural gas at transport conditions. We have investigated the case study involving using the separated CO₂ for simultaneous safe long-term storage of CO₂ and release of methane for in situ hydrates located at the North Makassar Basin in offshore Indonesia. Utilization of CO₂ will require additive gases to increase gas permeability and reduce the blocking of sediments by new CO₂-dominated hydrate. This analysis was conducted for variable content of nitrogen and H₂S. We have concluded that the water dew-point-based method appears to severely underestimate the risk of hydrate formation; the maximum water concentration it allows in gas will be larger by a factor of eighteen than the one permitted by approaches that used water adsorption on hematite (rust) as the criterion.

Nomenclature

T	Temperature [K]
T_c	Critical temperature [K]
P	Pressure [bar or kPa]
μ	Chemical potential [kJ/mol]
H	Hydrate phase
ΔG	Free energy change
G	Free energy change [kJ/mol]
P	Parent phase
R	Universal Gas Constant [kJ/(K mol)]
\varnothing	Fugacity coefficient
γ	Activity coefficient
\bar{x}	Mole fraction of liquid
\bar{y}	Mole fraction of gas

h_{ij}	Canonical cavity partition function of component j in cavity type i
Δg_{ij}^{inc}	Free energy of inclusion of the guest molecules j in the cavity i
θ_{ij}	Filling fraction of component j in cavity type i
β	Inverse of gas constant times temperature
x_T	Total mole fraction of all guests in the hydrate

1 Introduction

Hydrocarbons being transported to the processing plant for treatment are always accompanied by reservoir water. Under certain conditions, the water presence in natural gas mixtures during processing and transport gives rise to serious hydrate formation concerns. At high pressures and low temperatures, it can be thermodynamically beneficial for water molecules to form ice-like lattices (three-dimensional structures) with cavities encaging molecules of hydrocarbons and volatile liquids as well as certain inorganics like carbon dioxide and hydrogen sulphide (guest molecules). The resulting nonstoichiometric crystalline compounds are often referred to as clathrate

✉ Tatiana Kuznetsova
tatyana.kuznetsova@uib.no

¹ Department of Physics and Technology, University of Bergen, Allégaten 55, 5007 Bergen, Norway

hydrates or natural gas hydrates. Hydrate can grow to plug processing equipment and transport pipeline. In this work, we have evaluated the risk of hydrate formation based on the upper limit of water content that can be permitted in a multicomponent natural gas mixture with substantial amount of carbon dioxide. The Natuna gas field contains more than 70% of CO₂ and as such makes for a good case study of hydrate formation risk during the transport of CO₂ and hydrocarbons. The potential for simultaneous utilization and safe long terms storage of CO₂ in the natural gas hydrate coastal fields of Indonesia is a fascinating opportunity.

Several unit operations commonly employed in natural gas processing involve thermodynamic conditions that could give rise lead to hydrate formation. Processes that lead to increasing pressure and/or decreasing temperature can in many cases bring the fluid phases (CO₂, hydrocarbons) into hydrate formation region if free water is either available outright or can drop out from the fluid. Examples are turbines where gas expands and cools down, as well as low-temperature separators and compressors. The Natuna field has the advantage of not being very far from mainland Indonesia. From a long-term production perspective, 700 miles of pipeline transport for utilization and storage of CO₂ is certainly economically feasible. Moreover, the presence of offshore methane hydrates fields provides a storage option for the excessive CO₂ produced by the gas field. The seafloor temperatures in the area between Natuna and mainland Indonesia typically vary between 274 K and 283 K, with the pipeline transport from Natuna to onshore Indonesia involving pressures between 50 and 300 bars. A substantial portion of this thermodynamic range will fall inside the hydrate formation zone if free water becomes available by either dropping out from as liquid water or being adsorbed on rusty pipeline walls. A direct hydrate formation from water dissolved in fluid is possible but highly unlikely due to substantial limitation in mass transport and transport of released heat. As will be discussed in more detail later, studies available in open literature indicate that the presence of hematite significantly lowers the level of water tolerated during transport without invoking the risk of hydrate formation.

Determining the maximum water tolerance for gas being processed or transported is one of the critical parameters when it comes to design of drying facilities, whether solvent based (glycols is most common) or adsorption based (zeolites for instance).

Hydrate formation occurring in a system composed of natural gas with substantial admixture of impurities, for example water and carbon dioxide, will be a complex process involving competition between different phase transition mechanisms and routes, with both kinetics and thermodynamics playing significant roles. Conventional techniques currently used in industry to evaluate the risk of hydrate formation assume that hydrate will form when water drops out of the gas stream during processing or transport. Therefore, this method involves estimating the dew-point temperature of natural gas

mixtures in question. We refer to this approach as water drop-out or dew-point route to hydrate formation. However, the problem with this approach is that absolutely disregards that the presence of rust on the inside of pipeline walls and processing equipment will provide sites for water adsorption and consequently offer an alternative route for hydrate formation (the hematite route, hematite being the most dominant and one of the most thermodynamically stable forms of rust).

The problem grows in complexity [1] due to the fact that in an industrial setting like pipeline transport and processing, hydrate formation from natural gas cannot successfully attain equilibrium, as a result of limitations imposed by either Gibbs phase rule or mass and heat transport. The Gibbs phase rule is given as: $\tau = n - \pi + 2$. Here, τ refers to the degrees of freedom, which is the number of defined independent thermodynamic variables in the system, and π represents the number of actively coexisting phases, while n is the number of active components in terms of hydrate phase transitions. If we choose a simple scenario with only a single hydrate forming guest molecule present in the system containing bulk gas and water, say methane and water, with the existence of a hydrate nucleus, we will have three actively coexisting phases ($\pi = 3$) and two actively components ($n = 2$). And according to the Gibbs phase rule, the degrees of freedom should be just one ($\tau = 1$) for the system to reach equilibrium. But the system will never attain equilibrium because for a real industrial case involving flowing stream, hydrodynamics and hydrostatics including phase transitions which involves heat exchange, the fact that local pressure and temperature are specified. This means that even the simplest system with one guest molecule equilibrium (methane) can never achieve equilibrium. Furthermore, mass transport limitation and low concentration of water in methane could hinder hydrate crystal nucleus from ever attaining the critical size, thus preventing stable growth from even commencing.

Heat transport is yet another problem that can compound the issue of hydrate growth. Methane is a bad thermal conductor compared to liquid water clusters and hydrate before hydrate is formed [1], this means that transporting the exothermic heat of hydrate formation away from the system will become a challenge that could also critically restrict hydrate formation rate. Solid surfaces will also indirectly affect formation of hydrate; for instance, hydrate formation occurring on the interface between methane-rich gas and the aqueous phase adsorbed on solid wall surfaces covered with rust. This possible impact of water-wetting surfaces on the phase transitions should not be ignored just because the gas phase will dominate as far as the mass is concerned [1]. Hydrate nucleation and growth may take place either when both water and hydrate formers are adsorbed on the rusty surface or when water alone is present in the adsorbed phase, and hydrate former species are imported from the methane-rich phase. Hydrate formation will not occur directly on hematite surfaces due to

incompatibility between charge distribution in hydrate water lattice and hematite surface. Nevertheless, hematite will effectively function as a catalyst that removes water from the bulk gas via adsorption, thereby providing a separate water phase for hydrate formation, which will occur just outside the first two or three tightly structured water layers.

Thermodynamically, there exists a third possible pathway to hydrate formation. It involves hydrate forming directly from water dissolved in the natural gas stream. But the low concentration of water in the bulk gas combined with heat and mass transport limitations will make it highly improbable for hydrate to form via this pathway. Therefore, this alternative pathway has been left out of consideration in this work. Nevertheless, if surface stress from flow does not impact on water/hydrocarbon system at all, a quick formation of hydrate film on the water/hydrocarbon interface can take place, which will very rapidly block further transport of molecules of hydrate formers and waters through the hydrate film (extremely low diffusivity). Therefore, hydrate will form from the hydrate formers dissolved in water, and could also form from water dissolved in gas, which then would take advantage of nucleation on the hydrate surface. However, in case of flow with turbulent shear forces present, this situation is not feasible. Another difference between a flowing case and a case of a stationary constant volume and constant mass laboratory experiment is that new mass is supplied continuously. Consequently, the limiting situation where the water is completely consumed thus stopping hydrate formation will never happen.

This paper presents the application of our novel thermodynamic scheme for investigation of different routes to hydrate formation, utilizing ideal gas as reference state for all components in all phases including hydrate phase. We apply this scheme to determine the upper limit of water content that could be tolerated in a multicomponent natural gas with a substantial amount of CO₂ (Natuna gas as a case study) without the risk of hydrate formation during processing and transport. Two alternative pathways to hydrate formation, the traditional dew-point route approach and that facilitated by water adsorption on hematite-covered surfaces inside process equipment and pipeline are discussed below.

Using CO₂ for simultaneous safe long terms storage of CO₂ and release of methane from *in situ* hydrates is one alternative use for the substantial amount of CO₂ produced at the Natuna field. The conversion between methane hydrate and CO₂-dominated hydrate is made viable by two primary mechanisms. A solid-state exchange is possible but will be extremely slow and

Table 1 Composition of the original gas from Natuna gas-field

Gas	Mole fraction
CO ₂	0.710
CH ₄	0.270
C ₂ H ₆	0.010
N ₂	0.010

Table 2 Composition of the CH₄-rich gas stream

Gas	Mole fraction
CH ₄	0.940
C ₂ H ₆	0.035
CO ₂	0.025

thus of limited practical importance. The second mechanism will involve the formation of new hydrate from injected CO₂, with heat released by the formation process assisting in dissociation of *in situ* methane hydrate. The formation of new hydrate from injected CO₂ will be an extremely fast process and can potentially plug the reservoir. In addition, the permeability of CO₂ injected into water wetting reservoir is quite low. One way to circumvent these limitations is to add nitrogen to the injection gas. For instance, injection gas used in the Ignik Sikumi experiment in Alaska [2] even consisted of 77.5% N₂ by volume. A drawback of adding such high fraction of N₂ is the dramatic impact it can have on the thermodynamics of new CO₂ hydrate formation. In the worst-case scenario, the injection mixture may become too lean in CO₂ to create a new hydrate. In this limit, the system will have to proceed via the very slow solid-state exchange process, while a number of other phase transitions contributing to dissociation of in-situ methane hydrate may occur in the meantime. These transitions include hydrate dissociation when exposed to a N₂ rich phase and water under-saturated with methane. A substantial portion of accumulated methane released in the above-mentioned pilot experiment was likely due to the pressure reduction period. It is therefore hard to extract from the data how much CH₄ that were converted due to CO₂. In view of the low concentrations of CO₂ in the injected gas and other phase transitions that consume CO₂ (solution in water, adsorption of CO₂ on minerals). Various laboratories around the world has also conducted experiments on the exchange process but experimental set-up and conditions are frequently far away from a real situation in nature, including the fact that most of these available experimental data were conducted in equipment with tight temperature control. Since the most efficient conversion mechanism involves the formation of a new hydrate and dissociation of the methane hydrate due to released heat from this new formation of CO₂ dominated hydrate. Heat exchange with an external cooling system will therefore interfere with the natural mechanism. On top of this there are all the usual limitations of imitating a natural hydrate system which exposed to flow (diffusion to hydrodynamics depending on connection to fracture systems),

Table 3 Composition of the CO₂-rich gas stream

Gas	Mole fraction
CO ₂	0.982
N ₂	0.014
CH ₄	0.004

geochemistry and fluid/hydrate/mineral interactions which are different from the experimental set-up. And since these hydrate systems can never reach thermodynamic equilibrium they exist in a stationary state that has developed over geological time scales that is impossible to reproduce over limited time in a laboratory set-up.

The second part of this study has been therefore focused on the examination of thermodynamic stability limits governing the formation of hydrate from various mixtures of CO_2 and N_2 as related to a particular hydrate field example in offshore Indonesia. A comprehensive examination of all of the hydrate occurrences in that area lay well beyond the scope of this work; our choice of example also reflects the varying scope and quality of data available in the open literature.

2 Natuna gas reservoir

The gas composition of the Natuna Gas Reservoir is dominated by a very high content of CO_2 . According to [3], the gas consists of approximately 71% carbon dioxide, 27% methane, 1% ethane and heavier hydrocarbons (approximated as ethane), and 1% nitrogen and hydrogen sulphide combined. While hydrogen sulphide is an aggressive hydrate former, a tiny fraction of H_2S (less than 1%) will have only a limited impact on either the water dew-point and the maximum water content before drop-out due to adsorption on hematite. Rough estimates of conditions relevant for transport from Natuna to onshore Indonesia indicate that temperatures (below 280 K for seafloor pipeline transport) and pressures (between 50 and 300 bar) will fall inside the hydrate formation region. A critical question thus arises concerning the lowest fraction of water that will trigger either water condensation or adsorption on rusty pipe walls. In view of this, Table 1 presents gas composition chosen to model the gas stream being transported to land for separation.

Typically, the maximum CO_2 content of sales gas is limited to 2.5%. The acceptable loss levels of hydrocarbons in the separated CO_2 stream will be highly dependent on the separation method and costs versus increased value per extra unit of methane recovered. It will be desirable to separate as much of the methane as possible from the other gasses. Assuming that all N_2 will follow CO_2 , and all ethane will follow the CH_4 -rich phase resulted in the model systems for separated phases given in Tables 2 and 3 below.

3 Fluid thermodynamics

In equilibrium, temperatures, pressures, and chemical potentials of all coexisting phases must be the same across all phase boundaries. Though the equilibrium is unattainable in practice, applying a quasi-equilibrium method will help us to

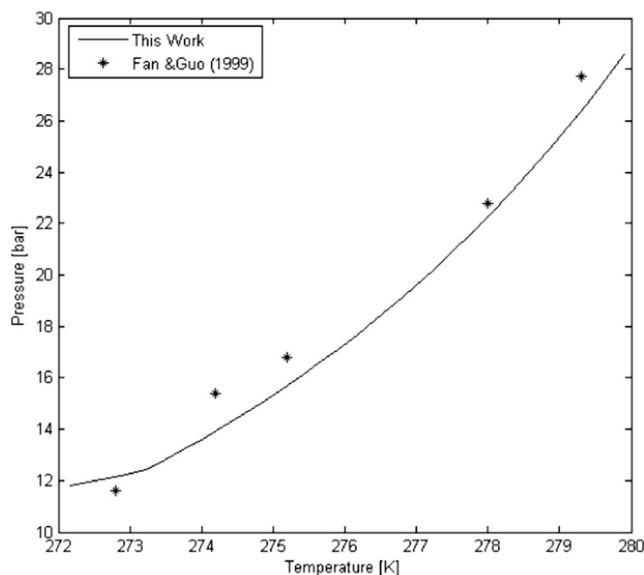


Fig. 1 Estimated equilibrium pressures for hydrate formed from a gas mixture containing 88.53 mol% of CO_2 , 6.83 mol% of CH_4 , 0.38 mol% C_2H_6 and 4.26 mol% of N_2 compared to experimental data [11]

evaluate the thermodynamic advantages of different pathways to formation/dissociation of hydrate as asymptotic stability limits for each given phase transition. The residual thermodynamics approach will be applied for all components and all phases (hydrate, liquid water, aqueous phases, ice) through the use of the Soave–Redlich–Kwong (SRK) equation of state [4]. Parameters required by the SRK have been mostly supplied by molecular dynamics simulations involving water in different phases (empty hydrates, liquid water, and ice) [5].

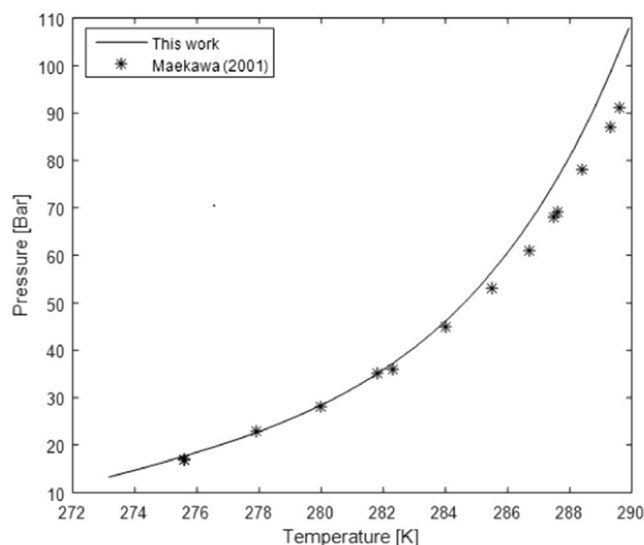


Fig. 2 Estimated equilibrium pressures for hydrate formed from a gas mixture containing 90.2 mol% of CH_4 and 9.8 mol% of C_2H_6 compared to experimental data [12]

In equilibrium systems, both phase distributions and compositions can be evaluated by means of free energy minimization. Provided that thermodynamic models are available, it is not a critical issue to choose a reference state for different components in different phases for equilibrium systems. However, in non-equilibrium systems, the most favourable local phase distributions, together with the thermodynamic driving forces encouraging each component to move across the phase boundaries from one phases to another can be determined by a free energy analysis. It is convenient in this case to use ideal gas as the reference state to ensure same reference values for free energy of every phase present in the estimation of the chemical potential of all components, irrespective of the phase as presented in Eq. (1):

$$\mu_j(T, P, \vec{y}) - \mu_j^{ideal\ gas}(T, P, \vec{y}) = R.T.\ln\phi_j(T, P, \vec{y})$$

$$\lim(\phi_i) \rightarrow 1.0 \dots \text{for ideal gas} \quad (1)$$

Where ϕ_i refers to the fugacity coefficient for component j in given phase; \vec{y} is the gas mole fraction vector. The chemical potential of the ideal gas comprises the trivial mixing term since ideal gas mixing of gases at constant pressure.

Another reference state is used to evaluate the chemical potential of component j as an intermediate step for the liquid state. It is given in Eq. (2) below generally known as symmetric excess. This equation involves the ideal liquid term (chemical potential) as well including the trivial ideal mixing term together with the pure liquid value.

$$\mu_j(T, P, \vec{x}) + \mu_j^{ideal\ liquid}(T, P, \vec{x}) = R.T.\ln\gamma_j(T, P, \vec{x})$$

$$\lim(\gamma_j) \rightarrow 1.0 \text{ when } x_j \rightarrow 1.0 \quad (2)$$

where γ_j is the activity coefficient for component j in the liquid mixture. When applying Eq. (2) to water, the ideal gas reference state can suitably be applied too when the chemical potential of pure liquid water is evaluated from molecular interaction models by means of molecular dynamics (MD) simulations. In this work we have utilized data from [5].

In case of gas components with low solubility in water, like the hydrocarbons in consideration, the “infinite dilution” of gas in water will make for a more suitable liquid reference state. Therefore, the asymmetric excess formulation in Eq. (3) will be appropriate. It is called asymmetric excess because the activity coefficient limit of the component j tends to one as the mole fraction vanishes as shown below:

$$\mu_j^{H_2O}(T, P, \vec{x}) + \mu_j^{H_2O, \infty}(T, P, \vec{x})$$

$$= R.T.\ln[x_j^{H_2O} \cdot \gamma_j^{H_2O, \infty}(T, P, \vec{x})] \lim(\gamma_j^{H_2O, \infty}) \text{ when } x_j \rightarrow 0 \quad (3)$$

Where $\mu_j^{H_2O}$ is the chemical potential of component j in water; ∞ stands for infinite dilution; $\gamma_j^{H_2O, \infty}$ is activity coefficient of component j in aqueous phase based on the same reference state; R is the universal gas constant. In practice, the evaluation of infinite dilution chemical potential with ideal gas as the reference state can be achieved by means of molecular dynamics (MD) simulations and application of the Gibbs–Duhem relation [6, 7], contingent on thermodynamic properties of all phases can also be specified and evaluated outside of equilibrium. The combination of the first and the second laws of thermodynamics requires that both available mass of every component as well as the overall mass will have to be distributed over all possible phases coexisting under specific local pressure and temperature conditions. This evaluation is quite straightforward for most of the fluid phases of interest, with the hydrate phase being somewhat an exception and needing a special consideration; it has however been comprehensively evaluated in Kvamme et al. [7, 8]. Thus, the minimization of free energy and obtaining values for the local phase distributions becomes possible through combining thermodynamic formulations for fluids in Eqs. (1), (2) and (3) with hydrate nonequilibrium formulations from Kvamme et al. [7, 8]. A number of algorithms capable of implementing this approach are available in the open literature.

Except for the hydrate phases, all the relevant pressures and temperatures will refer to a liquid state. All the situations considered in this work involve very low mutual solubilities and/or low concentrations. The following approximation in Eq. (4) should therefore prove satisfactorily accurate for most industrial applications where hydrate formation is a risk factor:

$$\mu_j^i(T, P, \vec{x}) \approx \mu_j^{i, \infty}(T, P, \vec{x})$$

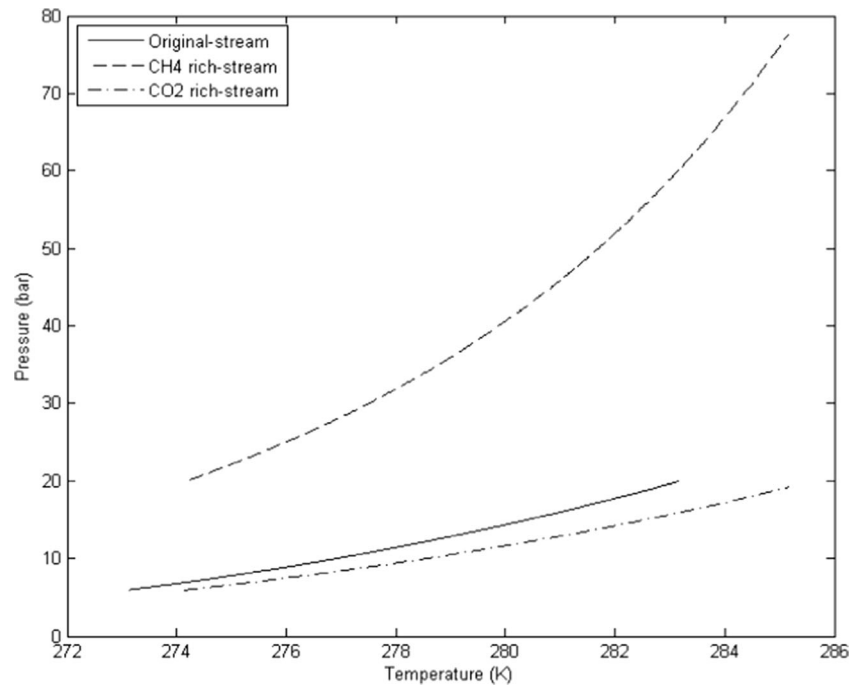
$$+ R.T.\ln[x_j^i \cdot \gamma_j^{i, \infty}(T, P, \vec{x})] \quad (4)$$

Here the subscript i distinguish between different phases with low solubility and subscript j refers to different components.

4 Thermodynamics of hydrate: model description and verification

The chemical potential of water in hydrate can be evaluated using the statistical mechanical model for water in hydrate, which is a typical Langmuir type of adsorption model. We used the version presented in Kvamme & Tanaka [5] given in Eq. (5). Unlike that of van der Waal and Platteuw (1959) [9], the Kvamme & Tanaka [5] form considers the lattice movements and corresponding effects of different guest molecules; it takes into account collisions between guest

Fig. 3 Hydrate equilibrium pressures for the original Natuna gas mixture (solid), CH₄-rich gas (dash) and CO₂-rich gas (dash-dot) streams



molecules and water sufficiently strong to affect the water motion. A rigid lattice is presumed by the van der Waal and Platteuw (1959) [9] model, it assumes that the guest j does not affect water movements in the lattice.

$$\mu_{H_2O}^{(H)} = \mu_{H_2O}^{(0,H)} - \sum_{i=1}^2 R.T.v_i \cdot \ln \left(1 + \sum_{j=1}^{n_{\text{guest}}} h_{ij} \right) \quad (5)$$

Fig. 4 Maximum concentration of water that can be permitted in Natuna gas before liquid water drops out. Curves from top to bottom correspond to pressure of 50 bar, 90 bar, 130 bar, 170 bar, 210 bar and 250 bar respectively

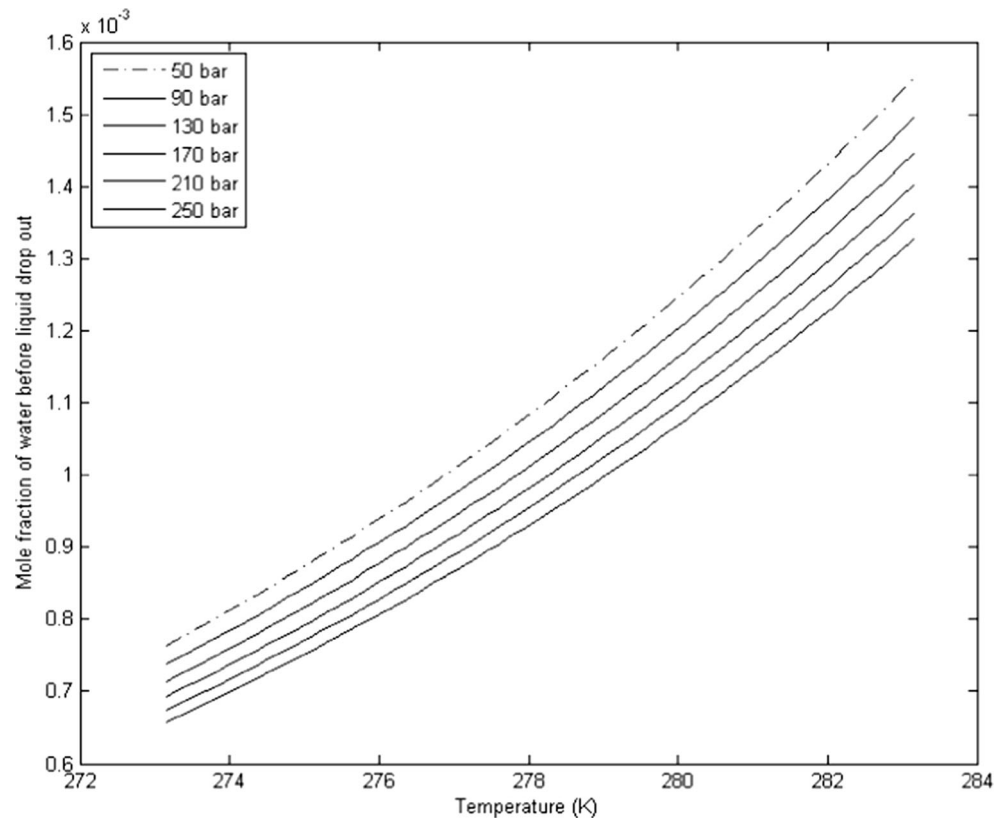
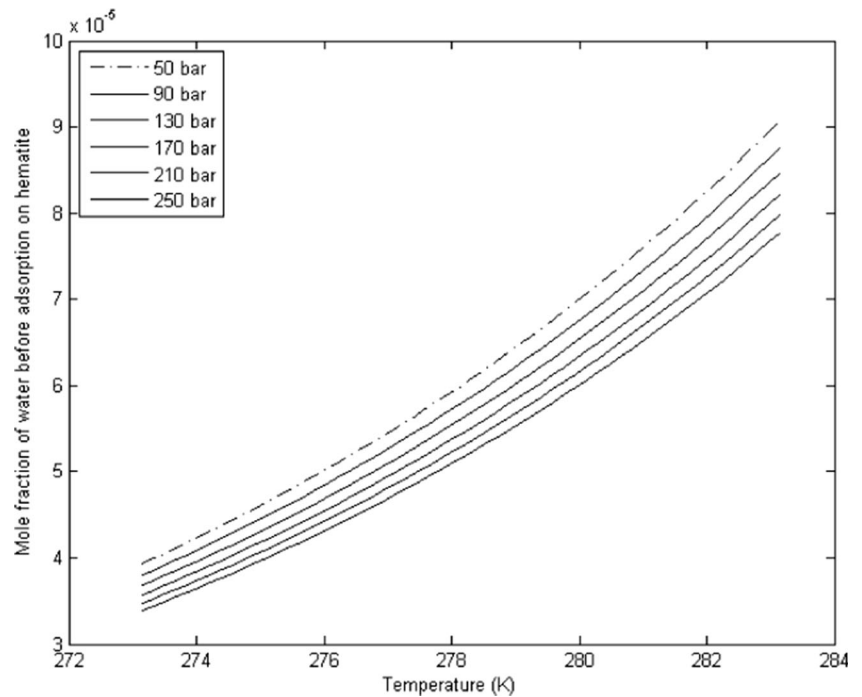


Fig. 5 Maximum concentration of water that can be permitted in Natuna gas before water is adsorbed on hematite. Curves from top to bottom correspond to pressure of 50 bar, 90 bar, 130 bar, 170 bar, 210 bar and 250 bar respectively



Where H denotes to hydrate phase; $\mu_{H_2O}^{(H)}$ refers to the chemical potential of water in hydrate; $\mu_{H_2O}^{(0,H)}$ is the chemical potential of water in empty clathrate structure; v_i refers to the fraction of cavity type i per water molecule. The unit cell of hydrate of structure I is composed of forty-six water molecules. Structure I hydrate has two small and six large cavities,

consequently, $v_{small\ cavity} = 1/23$ and $v_{large\ cavity} = 3/23$. h_{ij} is the canonical cavity partition function of component j in cavity type i . n_{guest} stands for number of guest molecules in the system. Equation (6) is used to evaluate the canonical partition function:

$$h_{ij} = e^{-\beta(\mu_i^H - \Delta g_{ij}^{inc})} \quad (6)$$

Fig. 6 Maximum concentration of water that can be permitted in the CH_4 -rich gas before liquid water drops out. Curves from top to bottom correspond to pressure of 50 bar, 90 bar, 130 bar, 170 bar, 210 bar and 250 bar respectively

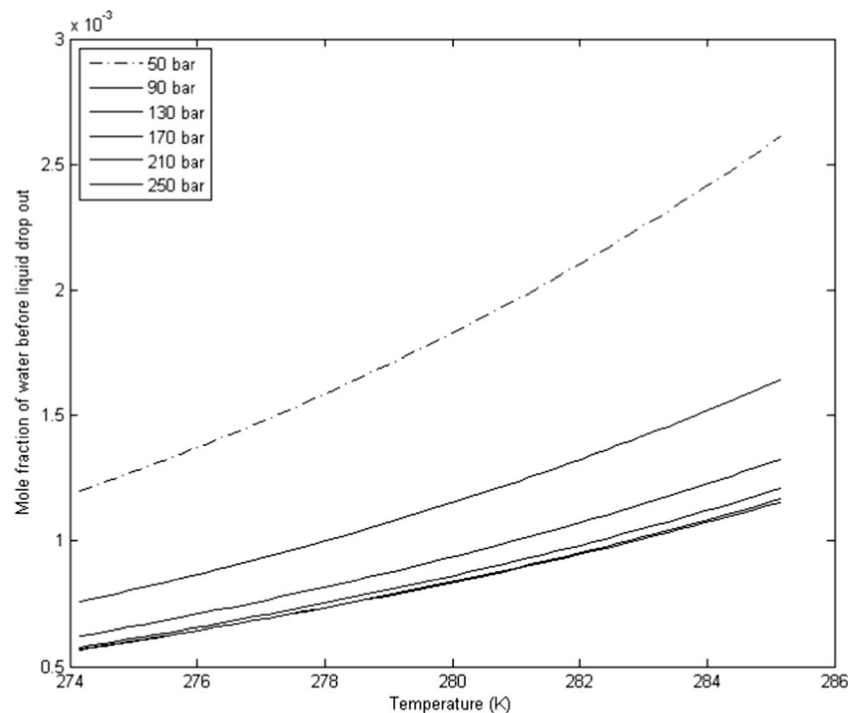
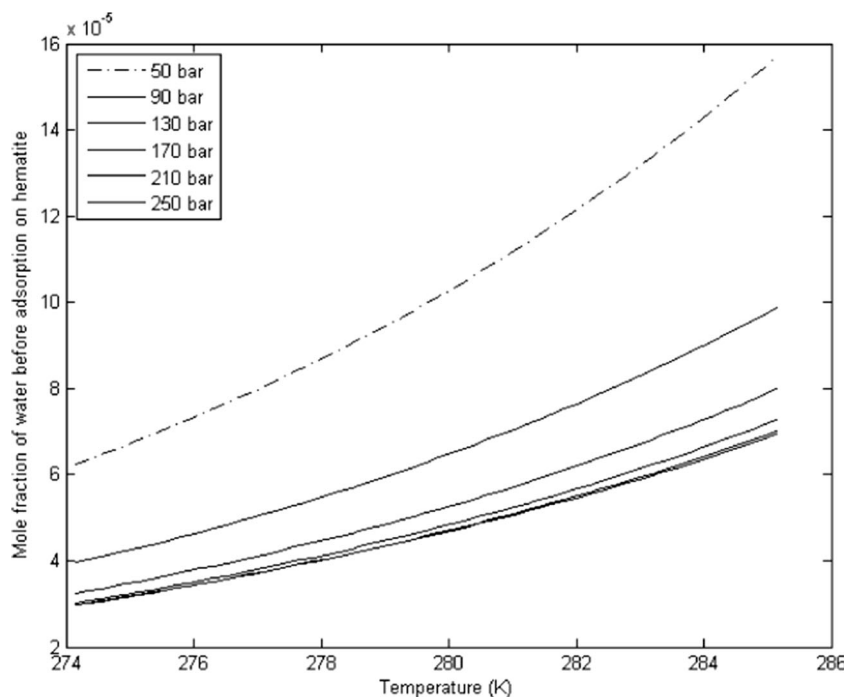


Fig. 7 Maximum concentration of water that can be permitted in the CH₄-rich gas before water is adsorbed on hematite. Curves from top to bottom correspond to pressure of 50 bar, 90 bar, 130 bar, 170 bar, 210 bar and 250 bar respectively



Here, β is the inverse of the product of gas constant and temperature, and Δg_{ij}^{inc} is the impact on hydrate water from inclusion of the guest molecules j in the cavity i [10]; its expansion coefficients are tabulated in Tables 4 and 5 below for carbon dioxide and hydrogen sulfide guests, respectively. In equilibrium, the chemical potential of component j in hydrate phase “ H ” must be identical to that in the (parent) phase from which it has been extracted [1]. Chemical potential of all gas components in hydrate are estimated by employing Eq. (1). The usual equilibrium approximation most hydrate simulators utilize is presented in Eq. (7) below assuming a free hydrate former phase (gas, liquid, fluid) in which every component’s chemical potential is generally estimated by an equation of state and the resulting chemical potential required in Eq. (6) for the cavity.

$$\begin{aligned} &\mu_{H_2O}^{(0,H)} - R.T \sum_{i=1}^2 v_i \ln \left(1 + \sum_{j=1}^{n_{guest}} h_{ij} \right) \\ &= \mu_{i,H_2O}^{Pure\ water}(T, P) + RT \ln \left[x_{i,H_2O} \gamma_{i,H_2O}(T, P, \vec{x}) \right] \end{aligned} \quad (7)$$

The estimation of the chemical potential of water in empty chlatrate (hydrate) structure has been implemented by means of Kvamme and Tanaka model [5]. This model has been proven to have predictive capabilities; consequently, it makes any empirical formulations for these chemical potentials unnecessary and possibly also nonphysical since chemical potential is a fundamental thermodynamic property. Given that the aqueous phase water lacks any ions and includes only limited amount of dissolved gases, the right-hand side of Eq. (7) has been approximated by the pure water value. This involves only a minor shift in chemical potential of liquid water. For instance, at 15000 kPa and 274 K

Table 4 Coefficients of $\Delta g_{inclusion}$ in the equation $\Delta g_{inclusion} = \sum_{i=0}^5 k_i \left[\frac{T_c}{T} \right]^i$ in case of CO₂ inclusion in structure I hydrate. Subscript c on T in the equation denote critical temperature. Critical temperature for CO₂ is 304.13 K. Units on k are in kJ/mol

k	Large cavity	Small cavity
0	1.624892126738541	-0.001472006897812825
1	1.163780531566063	-55.894438257553600
2	-56.736684127967590	-5.622310021096491
3	-27.993674783103930	19.483488092203920
4	16.859513200395660	11.325243831207700
5	19.774626541207180	3.033541053649439

Table 5 Coefficients of $\Delta g_{inclusion}$ in the equation $\Delta g_{inclusion} = \sum_{i=0}^5 k_i \left[\frac{T_c}{T} \right]^i$ for H₂S in structure I. Subscript c of T in the equation denote critical temperature. Critical temperature for H₂S is 373.0 K. Units of k are kJ/mol

k	Large cavity	Small cavity
0	16.016081922594900	-22.756290074587520
1	24.620388773936620	0.7857734898893513
2	-44.136111233969420	-33.910124845368450
3	-39.553535022042830	0.2509106251170165
4	2.362730250749388	-16.141504094980840
5	15.324247971160300	19.005383720423500

Table 6 The maximum concentration of water permitted in different gas-streams and comparing the two different routes to hydrate formation at a pressure of 250 bar

Pressure: 250 bar	Original gas		CH ₄ -rich gas		CO ₂ -rich gas	
	274 K	280 K	274 K	280 K	274 K	280 K
	Maximum mole fraction of water before liquid drop out ($\times 10^{-3}$)	0.701	1.078	0.569	0.836	0.564
Maximum mole fraction of water before adsorption on hematite ($\times 10^{-3}$)	0.036	0.061	0.030	0.047	0.029	0.047

the correction will be as small as -0.07 kJ/mol. Though slightly greater for 20,000 kPa and 25,000 kPa, it is still not dramatic for the purpose of this study. However, Eq. (8) has been proven to be beneficial to estimate free energy change corresponding to a hydrate phase transition Δg^H .

$$\Delta g^H = \delta \sum_{j=1}^{n^H} x_j^H (\mu_j^H - \mu_j^P) \quad (8)$$

Where H is refers to the hydrate phase of molecule j ; P is parent phase of molecule j . While Eq. (9) presents the relation between the filling fraction, the mole fractions and cavity partition function as shown below:

$$\theta_{ij} = \frac{x_{ij}^H}{v_j(1-x_T)} = \frac{h_{ij}}{1 + \sum_j h_{ij}} \quad (9)$$

Where x_T refers to the total mole fraction of all guests in the hydrate; θ_{ij} stands for the filling fraction of component j in cavity type i ; and x_{ij}^H is the mole fraction of component j in cavity type i .

Figures 1 and 2 present the comparison between the experimental data [11, 12] and hydrate equilibrium pressure-temperature curves estimated by our theoretical model for components relevant to this work: carbon dioxide, methane, ethane, and nitrogen. Rather than fitting the interaction parameters to replicate the experiment, our main goal was to ensure that the statistical-physics model of [5] was free of adjustable parameters in every term, including chemical potential of water in empty hydrate lattice, as liquid water, and in the form of ice. The comparison of our estimates with widely accepted experimental data demonstrates a quite satisfactory agreement without any

Table 7 Recapitulative table of pressure temperature and composition dependency for CO₂ hydrates formation and substitution in CH₄ hydrates structure I

Pressure [bar]	Fraction range	Minimal temperature required for (0.1) CO ₂ [K]
200	[0.1; 0.8]	277.0
210	[0.1; 0.8]	276.9
220	[0.1; 0.8]	276.7
230	[0.1; 0.8]	276.5
240	[0.1; 0.8]	276.3
250	[0.1; 0.8]	276.1

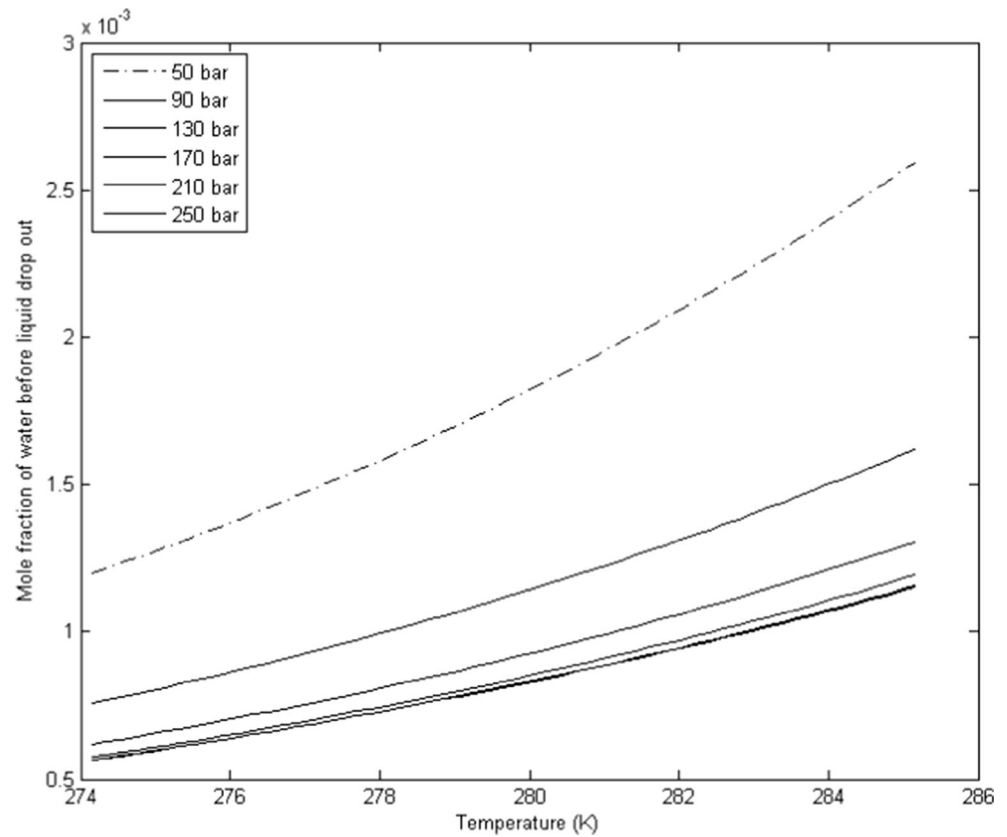
empirical fitting required. The slight deviation observed in Fig. 1 is due to guest-guest interactions for a quaternary gas mixture like the one in question. Figure 2 exhibits a very good match, especially inside the relevant temperature ranges of 273–286 K, which is just a binary gas mixture of methane and ethane. Therefore, we have deemed the deviations to be acceptable for the purposes of this work.

5 Hydrate risk analysis: alternative approaches for evaluating the risk of hydrate formation for Natuna gas from the reservoir

When hydrate risk under transport or processing is to be assessed for a particular gas mixture containing hydrate-forming hydrocarbons and inorganics (structure I components and CO₂ and in this study), the initial step is to evaluate the upper safe limit of water tolerated by the gas or liquid system before water will drop out as condensate. The classical approach to hydrate risk analysis involves evaluating the mole fraction of water in gas or liquid phase at the water dew-point. More recent analysis has been extended by considering two other alternative pathways [1, 7]. The first of these alternative pathways takes into account the process of water condensing out as adsorbed phase on the rusty (hematite) pipe walls. The other alternative route to hydrate formation considers hydrate forming directly from water dissolved in hydrate former phase. Despite the fact that the latter alternative route is thermodynamically feasible, it was associated with large mass- and heat-transport limitations in the hydrate forming systems examined in those studies [1, 7]. Thus, the route where hydrate forms directly from dissolved water will be extremely improbable compared to both the classical (dew-point) water drop-out approach and the alternative approach involving adsorption of water on hematite (rusty) surfaces. Therefore, our study ignored the third alternative and focused on the other two.

The produced gas transportation from Natuna gas-field will typically involve temperature 274 K to 283 K and pressures ranging from 50 to 300 bars. The processing conditions during separation onshore are not known since they are highly dependent on the separation methods. After the separation process on mainland, two new gas streams will be generated with compositions presented above in Tables 2 and 3. Both the CH₄- and CO₂-rich gas streams are expected to be transported

Fig. 8 Maximum concentration of water that can be permitted in the CO₂-rich gas before liquid water drops out. Curves from top to bottom correspond to pressure of 50 bar, 90 bar, 130 bar, 170 bar, 210 bar and 250 bar respectively



by pipeline operating at temperature and pressure ranging from 274 K to 285 K, and 50 bars to 250 bars, respectively.

Our novel thermodynamic scheme for investigation of different routes to hydrate formation, using ideal gas as reference

state for all components in all phases including hydrate phase has been applied to investigate the maximum limit of water content that should be permitted in Natuna gas from the Greater Sarawak Basin. Figure 1 presents the hydrate

Fig. 9 Maximum concentration of water that can be permitted in the CO₂-rich gas before water is adsorbed on hematite. Curves from top to bottom correspond to pressure of 50 bar, 90 bar, 130 bar, 170 bar, 210 bar and 250 bar respectively

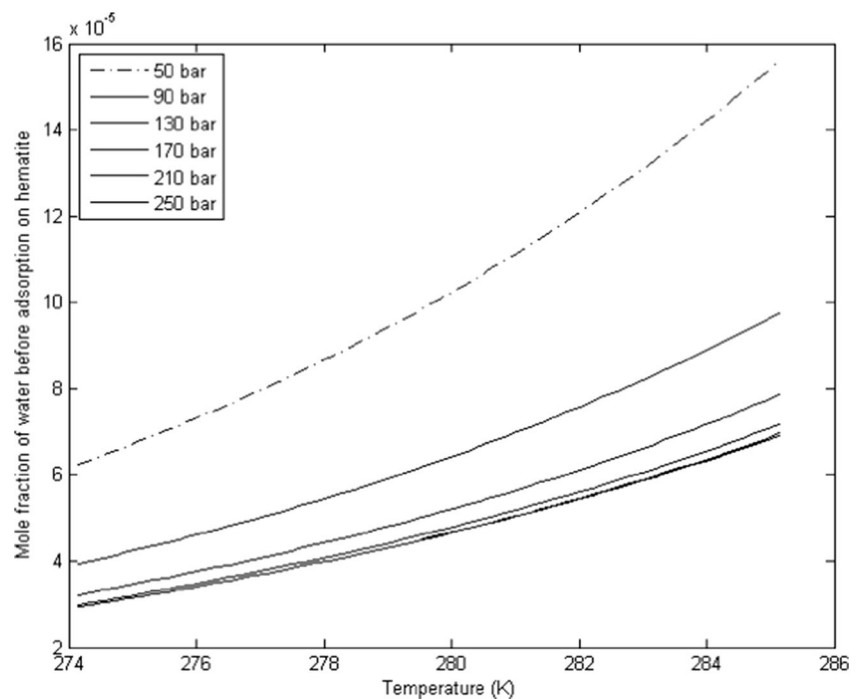
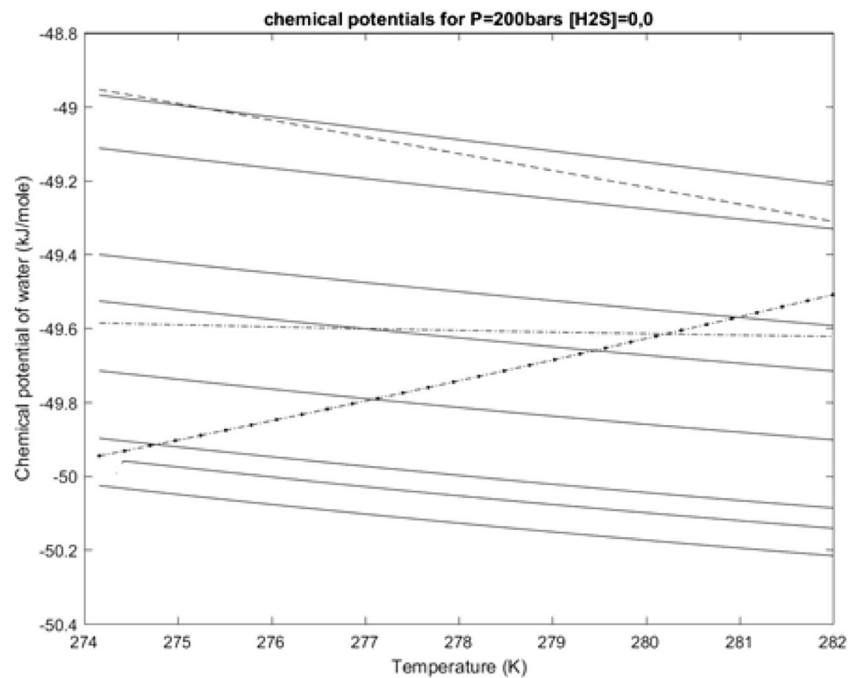
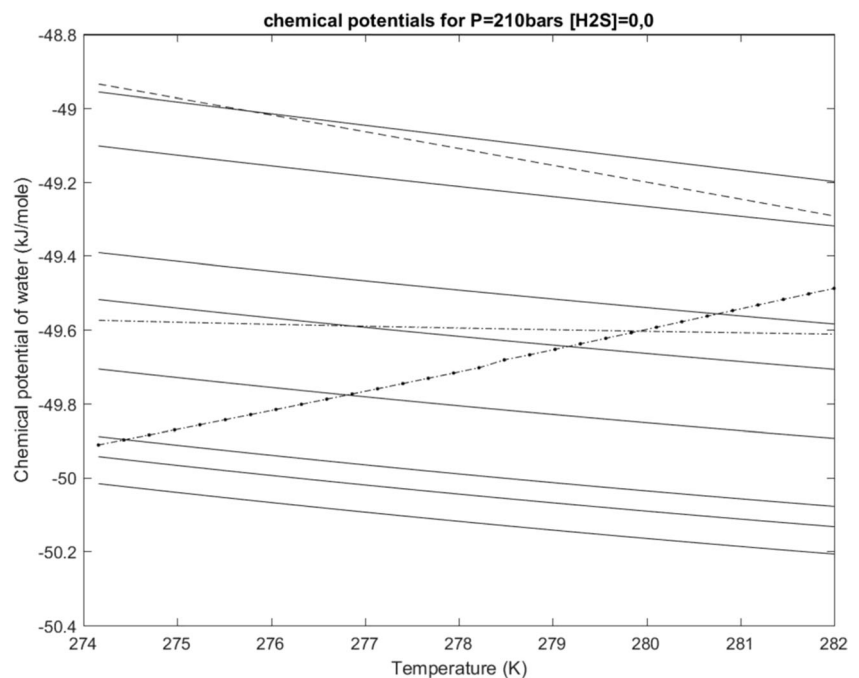


Fig. 10 Chemical potential as function of temperature of present components in the injection gas at $P = 200$ bar. The upper dashed curve is chemical potential of liquid water. The lower dashed curve is for chemical potential of water in methane hydrate. The dash-dot curve is the chemical potential of water in an artificial hydrate of structure II formed from a gas composition containing CH_4 , C_2H_6 and C_3H_8 . Solid curves are chemical potential for water in hydrate formed from various CO_2/N_2 ratios. Top curve is for a mole % of CO_2 of 1%. The following curves are for hydrate formed from a mole % of respectively 2, 5, 10, 20, 40, 60, 80% CO_2 from top to bottom



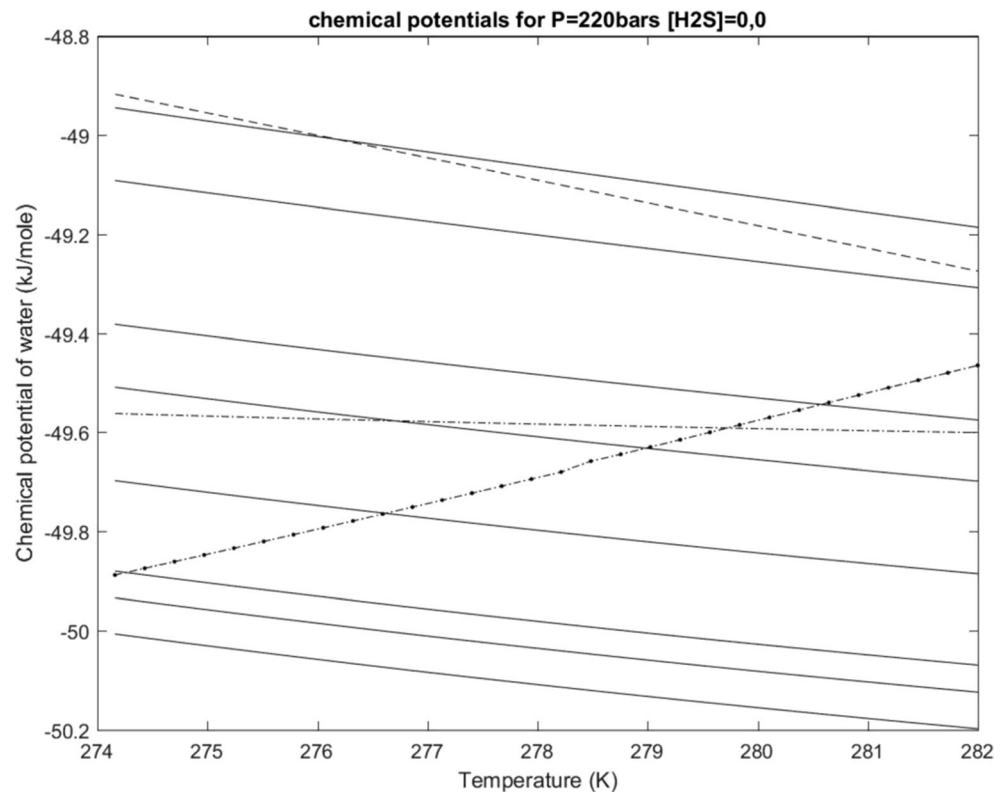
equilibrium curves for the three gas streams in question. Figures 2, 3, 4, 5, 6 and 7 illustrate qualitatively the safe limits of water content for Natuna gas before and after most of the CO_2 is separated out of the bulk, with both the classical dew-point liquid water drop-out approach and the alternative route involving adsorption of water on the rusty surfaces of process equipment and transport pipes. Maximum water level tolerated before water will start to drop out from the original gas from Natuna are plotted in Fig. 2. Levels calculated basing on adsorption on hematite is shown in Fig. 3 for the same gas.

Fig. 11 Chemical potential as function of temperature of present components in the injection gas at $P = 210$ bar. The upper dashed curve is chemical potential of liquid water. The lower dashed curve is for chemical potential of water in methane hydrate. The dash-dot curve is the chemical potential of water in an artificial hydrate of structure II formed from a gas composition containing CH_4 , C_2H_6 and C_3H_8 . Solid curves are chemical potential for water in hydrate formed from various CO_2/N_2 ratios. Top curve is for a mole % of CO_2 of 1%. The following curves are for hydrate formed from a mole % of respectively 2, 5, 10, 20, 40, 60, 80% CO_2 from top to bottom



Both the methane- and CO_2 -rich gas exhibit similar trends for all pressures presented in Figs. 4 to 7. Only a tiny shift in absolute values of water drop-out mole fractions is present, with methane values being slightly higher compared to CO_2 . Generally, both hydrate formation routes share a significant reduction in the gap/difference between the pressure curves between 50 bar and 90 bar, and between 90 bar and 130 bar. The curves for the two highest pressures, 210 bar and 250 bar, overlap for both methane and CO_2 . In case of the CO_2 stream, the pressure curves overlap

Fig. 12 Chemical potential as function of temperature of present components in the injection gas at $P = 220$ bar. The upper dashed curve is chemical potential of liquid water. The lower dashed curve is for chemical potential of water in methane hydrate. The dash-dot curve is the chemical potential of water in an artificial hydrate of structure II formed from a gas composition containing CH_4 , C_2H_6 and C_3H_8 . Solid curves are chemical potential for water in hydrate formed from various CO_2/N_2 ratios. Top curve is for a mole % of CO_2 of 1%. The following curves are for hydrate formed from a mole % of respectively 2, 5, 10, 20, 40, 60, 80% CO_2 from top to bottom



almost completely, indicating the higher density impact. The differences at the highest pressures are virtually insensitive to pressure due to the high density.

The safe-limit of water content decrease as the pressure increases for pure structure I hydrate components as methane and CO_2 . This is also the case original CO_2 -dominated Natuna

Fig. 13 Chemical potential as function of temperature of present components in the injection gas at $P = 230$ bar. The upper dashed curve is chemical potential of liquid water. The lower dashed curve is for chemical potential of water in methane hydrate. The dash-dot curve is the chemical potential of water in an artificial hydrate of structure II formed from a gas composition containing CH_4 , C_2H_6 and C_3H_8 . Solid curves are chemical potential for water in hydrate formed from various CO_2/N_2 ratios. Top curve is for a mole % of CO_2 of 1%. The following curves are for hydrate formed from a mole % of respectively 2, 5, 10, 20, 40, 60, 80% CO_2 from top to bottom

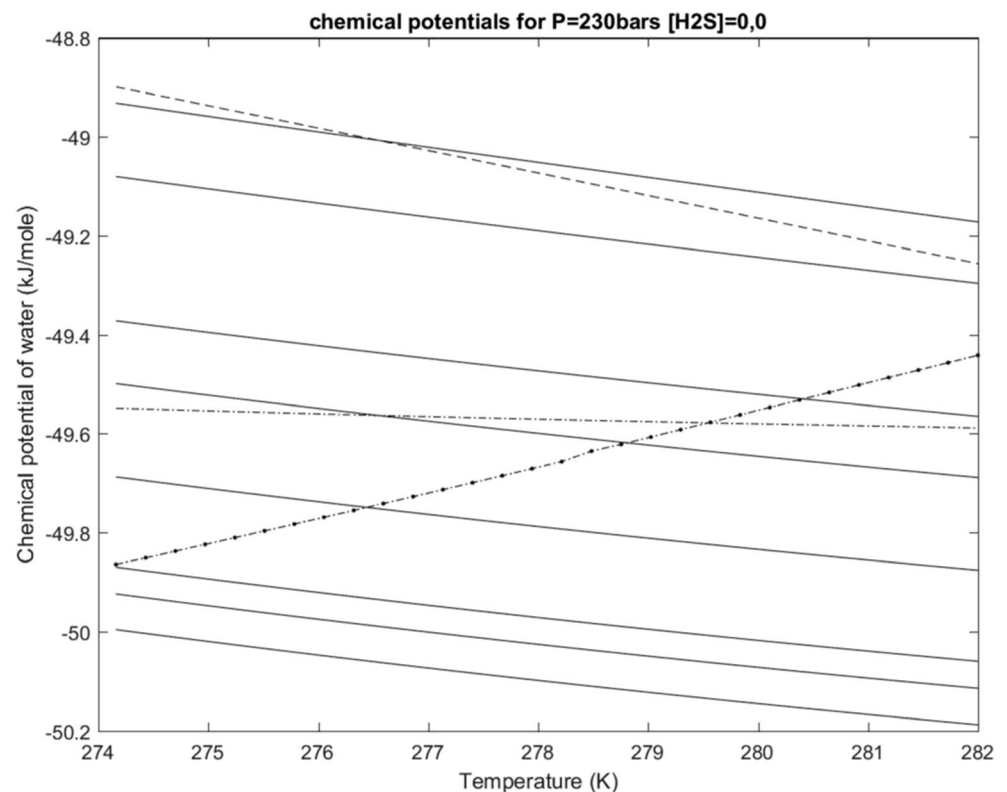
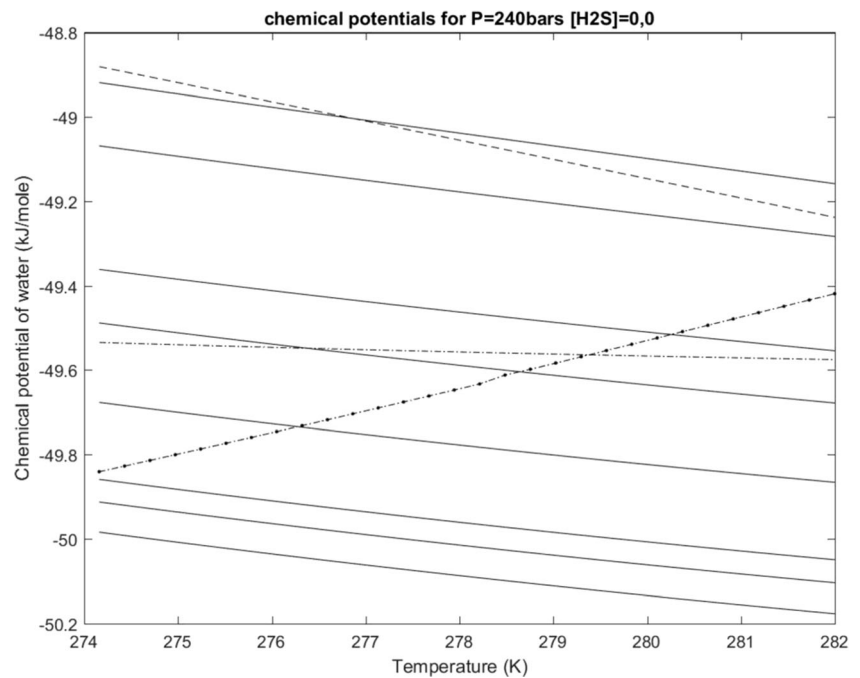


Fig. 14 Chemical potential as function of temperature of present components in the injection gas at $P = 240$ bar. The upper dashed curve is chemical potential of liquid water. The lower dashed curve is for chemical potential of water in methane hydrate. The dash-dot curve is the chemical potential of water in an artificial hydrate of structure II formed from a gas composition containing CH_4 , C_2H_6 and C_3H_8 . Solid curves are chemical potential for water in hydrate formed from various CO_2/N_2 ratios. Top curve is for a mole % of CO_2 of 1%. The following curves are for hydrate formed from a mole % of respectively 2, 5, 10, 20, 40, 60, 80% CO_2 from top to bottom



gas due to its lack of heavier hydrocarbons such as propane, and iso-butane etc.

When comparing safe water limit corresponding to the two hydrate formation routes in case of Natuna gas, the formation route that involves water adsorption on hematite yielded the water mole fraction which was by a factor of 19 smaller than value given by the classical dew-point approach currently used as industrial standard. This large

difference underlines the risk that hydrates may still form in industrial processes if only the dew-point approach is used as the hydrate safety criterion measure. Therefore, this alternative route involving adsorption of water on rusty surfaces and providing a free water phase for hydrate nucleation should not be ignored if the risk of hydrate formation without addition of inhibitions or applying other costly measures during processing and pipeline transport of

Fig. 15 Chemical potential as function of temperature of present components in the injection gas at $P = 250$ bar. The upper dashed curve is chemical potential of liquid water. The lower dashed curve is for chemical potential of water in methane hydrate. The dash-dot curve is the chemical potential of water in an artificial hydrate of structure II formed from a gas composition containing CH_4 , C_2H_6 and C_3H_8 . Solid curves are chemical potential for water in hydrate formed from various CO_2/N_2 ratios. Top curve is for a mole % of CO_2 of 1%. The following curves are for hydrate formed from a mole % of respectively 2, 5, 10, 20, 40, 60, 80% CO_2 from top to bottom

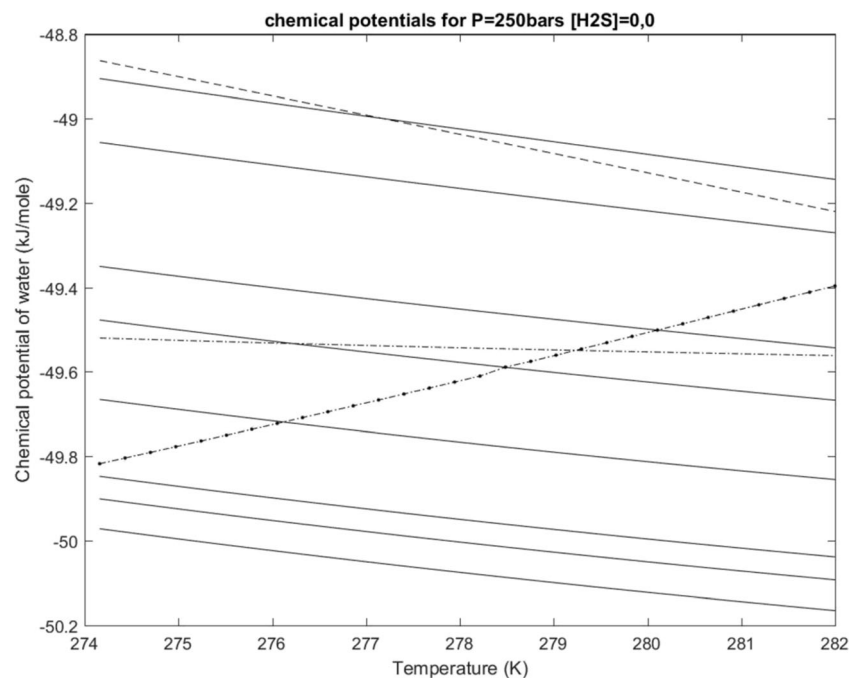
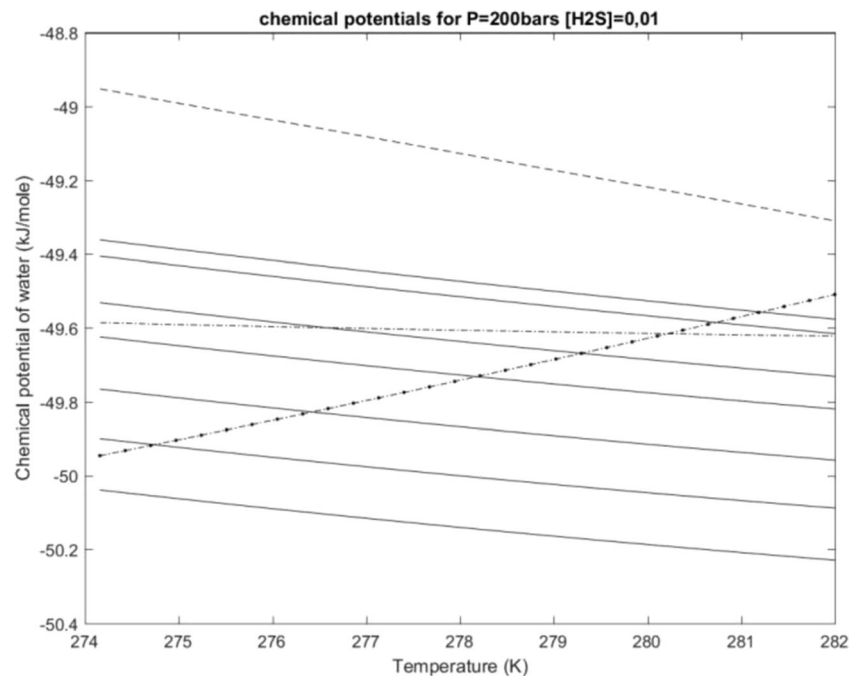


Fig. 16 Chemical potential as function of temperature of present components in the injection gas containing 1% H₂S at $P = 200$ bar. The upper dashed curve is chemical potential of liquid water. The lower dashed curve is for chemical potential of water in methane hydrate. The dash-dot curve is the chemical potential of water in an artificial hydrate of structure II formed from a gas composition containing CH₄, C₂H₆ and C₃H₈. Solid curves are chemical potential for water in hydrate formed from various CO₂/N₂ ratios. H₂S amount has been added directly as molar ratio and the composition has been normalized. Top curve is for a mole % of CO₂ of 1%. The following curves are for hydrate formed from a mole % of respectively 2, 5, 10, 20, 40, 60, 80% CO₂ from top to bottom



natural gas must be avoided. On the other hand, it is not possible for initial hydrate nuclei to attach directly to the rust surface due to the low chemical potential of adsorbed water. The hydrate formed will be bridged by at least three to four layers of structured water on the surface of the hematite. This alternative route to hydrate formation through adsorption on hematite absolutely dominates when it comes to the risk of water dropping out from gas mixture and pure components to form a separate water phase and

ultimately resulting in hydrate formation. This can be understood from the fact that the average chemical potential of water adsorbed on hematite could be 3.4 kJ/mol lower than that of liquid water. And thermodynamics does favour minimum free energy.

Table 6 presents the maximum amount of water tolerated in various gas streams calculated using coefficients provided in Tables 4 and 5. With anticipated transport pressures varying between 50 and 250 bars and the highest seafloor

Fig. 17 Chemical potential as function of temperature of present components in the injection gas containing 1% H₂S at $P = 210$ bar. The upper dashed curve is chemical potential of liquid water. The lower dashed curve is for chemical potential of water in methane hydrate. The dash-dot curve is the chemical potential of water in an artificial hydrate of structure II formed from a gas composition containing CH₄, C₂H₆ and C₃H₈. Solid curves are chemical potential for water in hydrate formed from various CO₂/N₂ ratios. H₂S amount has been added directly as molar ratio and the composition has been normalized. Top curve is for a mole % of CO₂ of 1%. The following curves are for hydrate formed from a mole % of respectively 2, 5, 10, 20, 40, 60, 80% CO₂ from top to bottom

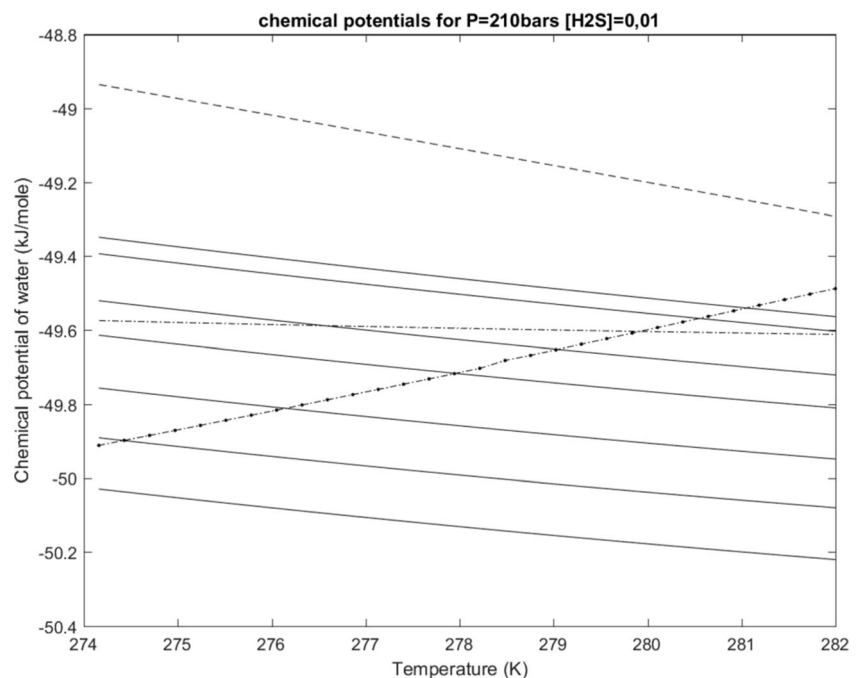
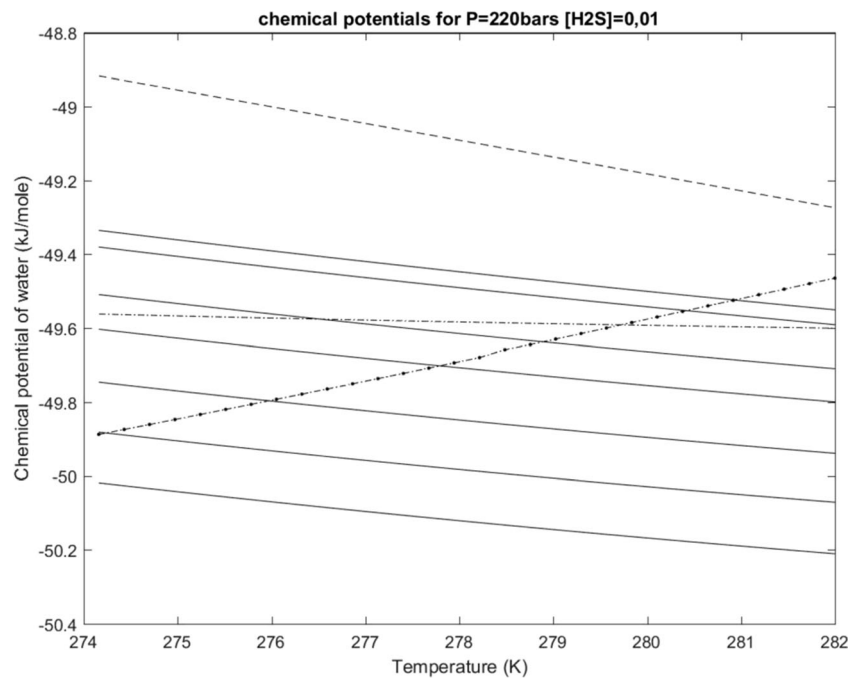


Fig. 18 Chemical potential as function of temperature of present components in the injection gas containing 1% H₂S at $P = 220$ bar. The upper dashed curve is chemical potential of liquid water. The lower dashed curve is for chemical potential of water in methane hydrate. The dash-dot curve is the chemical potential of water in an artificial hydrate of structure II formed from a gas composition containing CH₄, C₂H₆ and C₃H₈. Solid curves are chemical potential for water in hydrate formed from various CO₂/N₂ ratios. H₂S amount has been added directly as molar ratio and the composition has been normalized. Top curve is for a mole % of CO₂ of 1%. The following curves are for hydrate formed from a mole % of respectively 2, 5, 10, 20, 40, 60, 80% CO₂ from top to bottom



temperature around 6 degrees Celsius, it is obvious from Fig. 1 that all considered mixtures will exist inside the hydrate formation region. The question is therefore at which water concentrations in gas the water will drop out. Since the maximum pressure (Figs. 2 to 7) provides the estimate for the lowest of permitted gas in all systems, we have extracted some illustrative examples corresponding to that pressure.

Table 6 lists the maximum safe water limits permitted at two temperatures 274 k and 280 K and 250 bars.

As expected from earlier studies, water solubility are quite similar for both methane-rich and carbon dioxide-rich gas mixtures. The maximum amounts of water before liquid water drop-out or adsorption respectively are also quite similar for the two mixtures, in contrast to the original Natuna

Fig. 19 Chemical potential as function of temperature of present components in the injection gas containing 1% H₂S at $P = 230$ bar. The upper dashed curve is chemical potential of liquid water. The lower dashed curve is for chemical potential of water in methane hydrate. The dash-dot curve is the chemical potential of water in an artificial hydrate of structure II formed from a gas composition containing CH₄, C₂H₆ and C₃H₈. Solid curves are chemical potential for water in hydrate formed from various CO₂/N₂ ratios. H₂S amount has been added directly as molar ratio and the composition has been normalized. Top curve is for a mole % of CO₂ of 1%. The following curves are for hydrate formed from a mole % of respectively 2, 5, 10, 20, 40, 60, 80% CO₂ from top to bottom

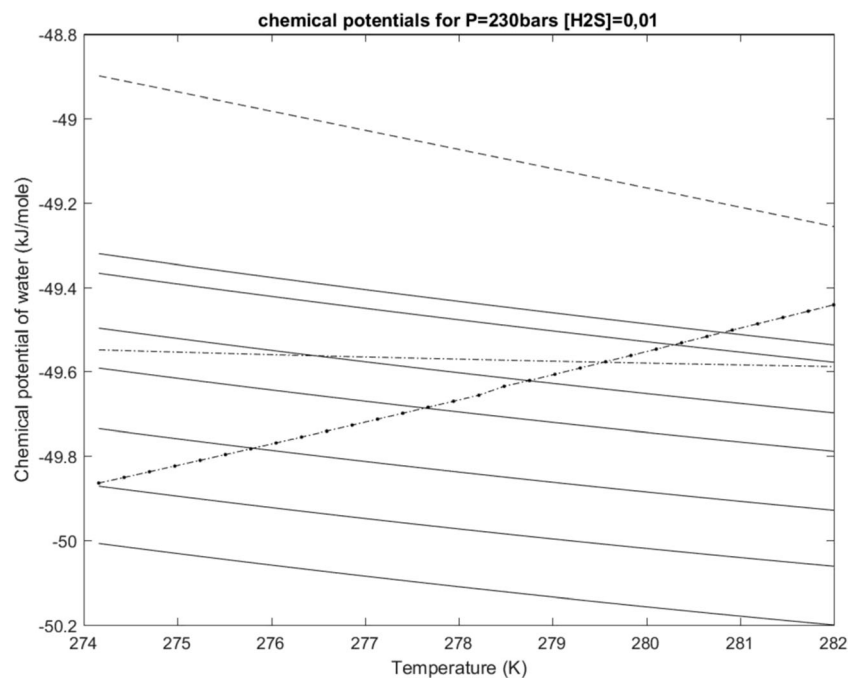
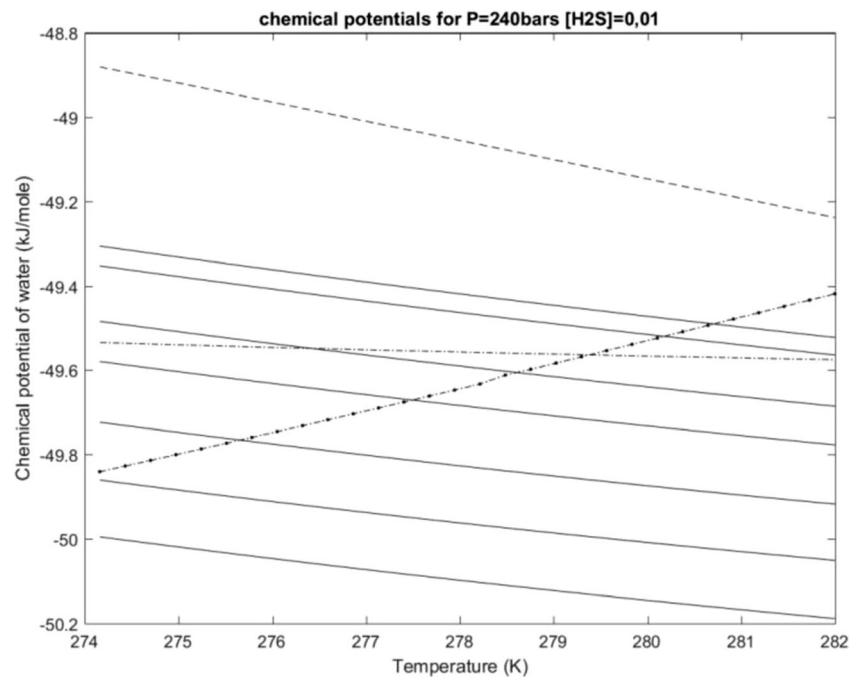


Fig. 20 Chemical potential as function of temperature of present components in the injection gas containing 1% H₂S at $P = 240$ bar. The upper dashed curve is chemical potential of liquid water. The lower dashed curve is for chemical potential of water in methane hydrate. The dash-dot curve is the chemical potential of water in an artificial hydrate of structure II formed from a gas composition containing CH₄, C₂H₆ and C₃H₈. Solid curves are chemical potential for water in hydrate formed from various CO₂/N₂ ratios. H₂S amount has been added directly as molar ratio and the composition has been normalized. Top curve is for a mole % of CO₂ of 1%. The following curves are for hydrate formed from a mole % of respectively 2, 5, 10, 20, 40, 60, 80% CO₂ from top to bottom



gas. In all cases, the maximum water tolerances based on the dew-point are in the order of 18 times higher that tolerance criteria based on Hematite adsorption.

6 A possible hydrate reservoir for CO₂ storage and utilization

While considering the production of natural gas from the Natuna field wells, it is extremely important to address the

high fraction of CO₂ (71 mol%) that this field contains. Given the impact of global warming and the focus on sustainable industry, the storage alternatives for such a huge amount of CO₂ must be carefully considered. Luckily, Indonesia is fortunate to have several huge methane hydrates fields that could serve as perfect storage options for CO₂ and a viable intermediary for the EOR.

The North Makassar Basin hydrate field is one of them, with a reasonable collection of seismic data available [12], making it a good case study to address the storage and utilization of carbon

Fig. 21 Chemical potential as function of temperature of present components in the injection gas containing 1% H₂S at $P = 250$ bar. The upper dashed curve is chemical potential of liquid water. The lower dashed curve is for chemical potential of water in methane hydrate. The dash-dot curve is the chemical potential of water in an artificial hydrate of structure II formed from a gas composition containing CH₄, C₂H₆ and C₃H₈. Solid curves are chemical potential for water in hydrate formed from various CO₂/N₂ ratios. H₂S amount has been added directly as molar ratio and the composition has been normalized. Top curve is for a mole % of CO₂ of 1%. The following curves are for hydrate formed from a mole % of respectively 2, 5, 10, 20, 40, 60, 80% CO₂ from top to bottom

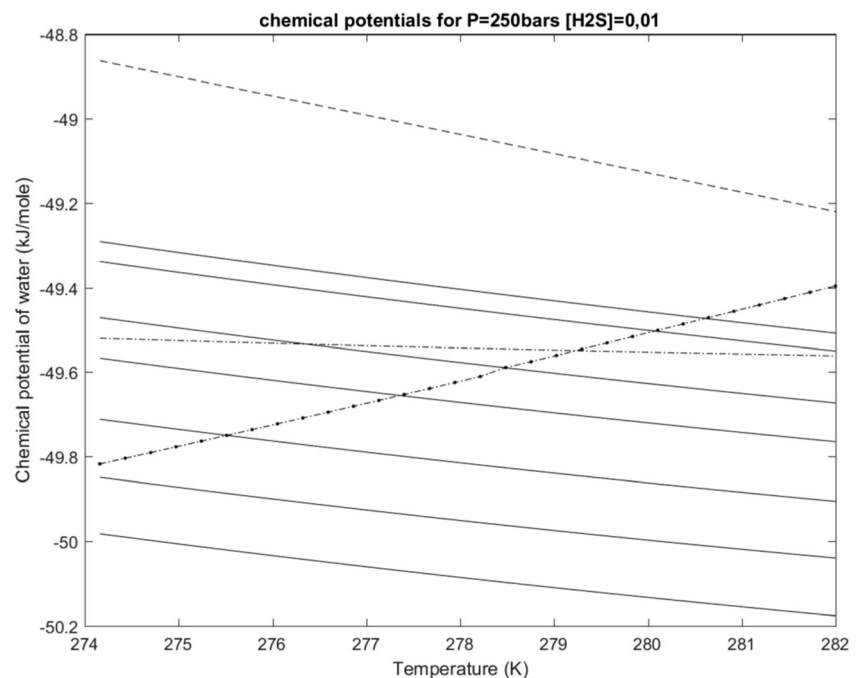
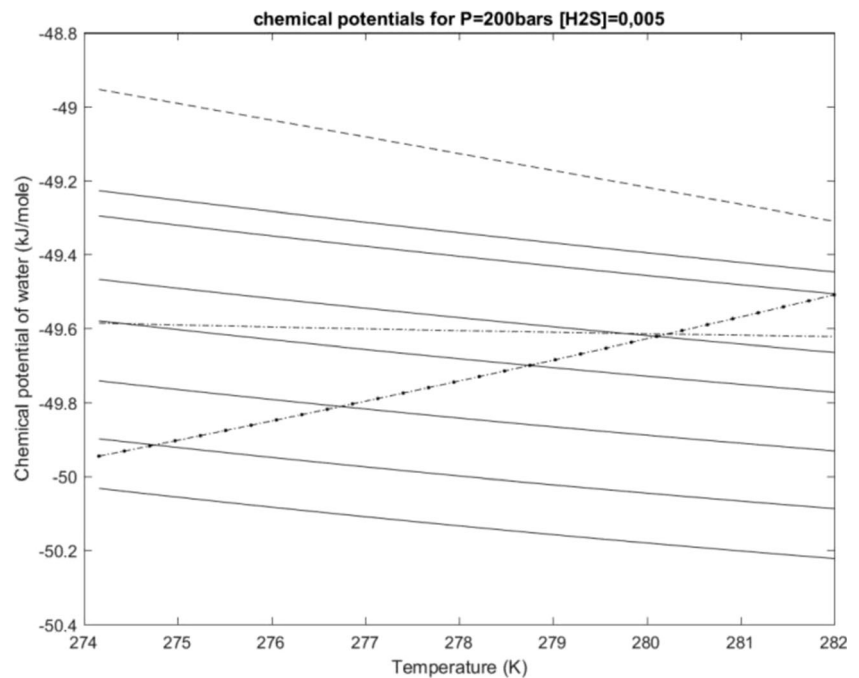


Fig. 22 Chemical potential as function of temperature of present components in the injection gas containing 0.5% H₂S at $P = 200$ bar. The upper dashed curve is chemical potential of liquid water. The lower dashed curve is for chemical potential of water in methane hydrate. The dash-dot curve is the chemical potential of water in an artificial hydrate of structure II formed from a gas composition containing CH₄, C₂H₆ and C₃H₈. Solid curves are chemical potential for water in hydrate formed from various CO₂/N₂ ratios. H₂S amount has been added directly as molar ratio and the composition has been normalized. Top curve is for a mole % of CO₂ of 1%. The following curves are for hydrate formed from a mole % of respectively 2, 5, 10, 20, 40, 60, 80% CO₂ from top to bottom



dioxide from Natuna. To be able to store CO₂ efficiently, CO₂ must be converted to hydrate. Indeed, in such a solid form, there are limited risks of leaks from the wells and pollution of the area.

Moreover, when it comes to EOR, combining the storage of CO₂ with recovery of almost pure methane is one of the best ways to go, provided that pressure and temperature of methane hydrate fields are suitable for CO₂ substitution in type I hydrate. The affinity of CO₂ for type I hydrate structures

is greater than that of CH₄ over pressure and temperature ranges easily achievable in the hydrates fields, thus allowing us to seriously consider the possibility of CO₂ storage.

Data collected by B. A. Jackson [13] show an 8000 m² area where several indicators point to potential presence of hydrates at approximate depth of 2450 m. Given the provided properties of seafloor and crust, it is possible to calculate pressure and temperature gradient in the field. Our calculations

Fig. 23 Chemical potential as function of temperature of present components in the injection gas containing 0.5% H₂S at $P = 210$ bar. The upper dashed curve is chemical potential of liquid water. The lower dashed curve is for chemical potential of water in methane hydrate. The dash-dot curve is the chemical potential of water in an artificial hydrate of structure II formed from a gas composition containing CH₄, C₂H₆ and C₃H₈. Solid curves are chemical potential for water in hydrate formed from various CO₂/N₂ ratios. H₂S amount has been added directly as molar ratio and the composition has been normalized. Top curve is for a mole % of CO₂ of 1%. The following curves are for hydrate formed from a mole % of respectively 2, 5, 10, 20, 40, 60, 80% CO₂ from top to bottom

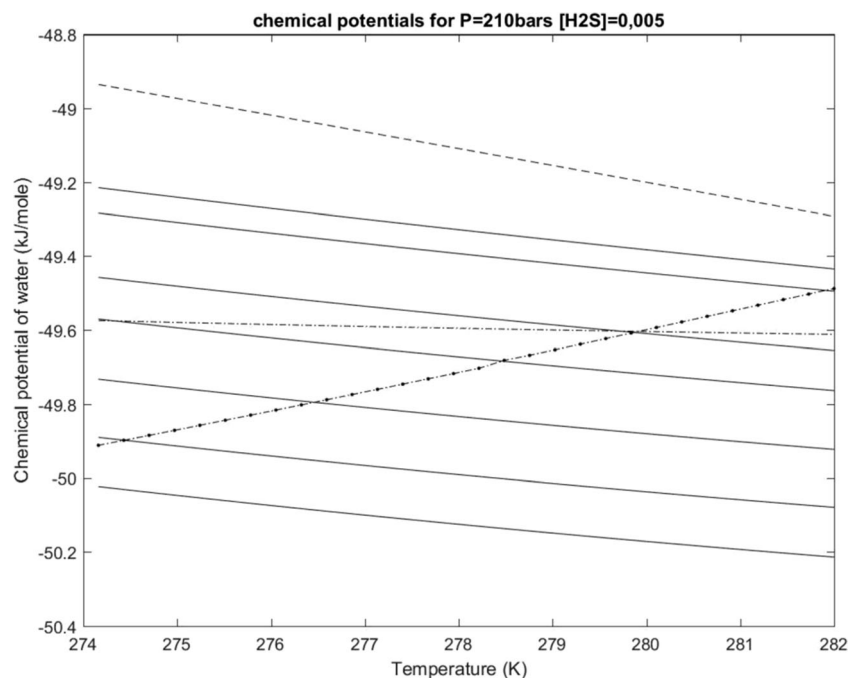
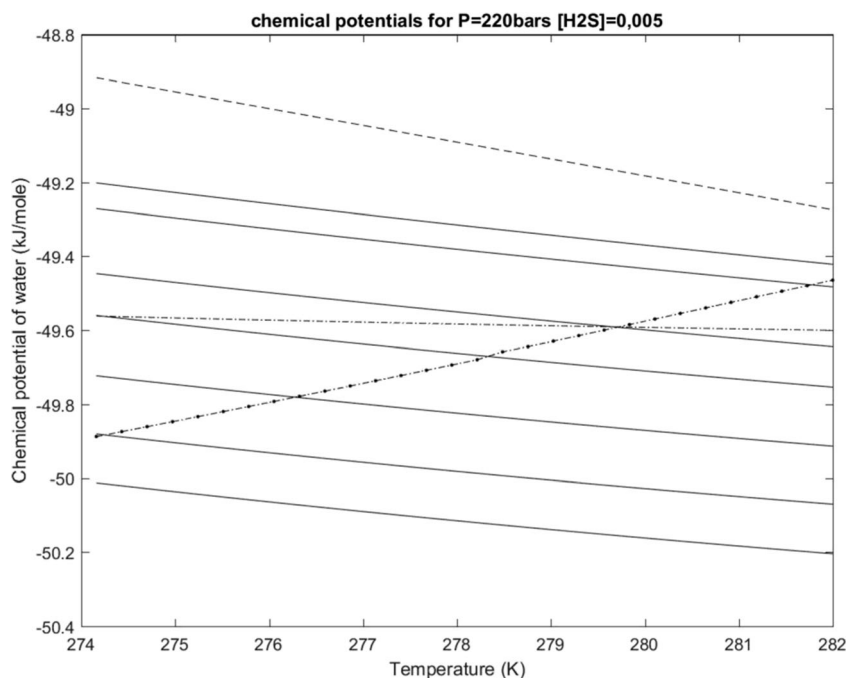


Fig. 24 Chemical potential as function of temperature of present components in the injection gas containing 0.5% H_2S at $P = 220$ bar. The upper dashed curve is chemical potential of liquid water. The lower dashed curve is for chemical potential of water in methane hydrate. The dash-dot curve is the chemical potential of water in an artificial hydrate of structure II formed from a gas composition containing CH_4 , C_2H_6 and C_3H_8 . Solid curves are chemical potential for water in hydrate formed from various CO_2/N_2 ratios. H_2S amount has been added directly as molar ratio and the composition has been normalized. Top curve is for a mole % of CO_2 of 1%. The following curves are for hydrate formed from a mole % of respectively 2, 5, 10, 20, 40, 60, 80% CO_2 from top to bottom



yielded the 200 bar - 250 bar pressure range and 274 K to 282 K temperature range, facilitating the estimation of chemical potential for the different relevant components. These results are plotted in Figs. 8, 9, 10, 11, 12, 13, 14, 15, 16, 17, 18, 19, 20, 21, 22, 23, 24, 25, 26 and 27 below, where the solid lines represent different concentration of CO_2 [CO_2] = 0.01; 0.02; 0.05; 0.1; 0.2; 0.4; 0.6; 0.8. The dashed line corresponds to water, the dot dashed line to methane hydrate structure I (the only one relevant in our case), and the

double dash dotted line to methane hydrate structure II. Analysis of the present figures show several points that should be highlighted.

As reservoir pressure increases, chemical potential of CO_2 becomes progressively lower, indicating easier CH_4 substitution by CO_2 , but we must exercise caution when it comes to the stability of CO_2 hydrates. Indeed, if CO_2 hydrate formation is too fast, it may seal off the reservoir close to the injection zone. CO_2 would then form hydrates directly from free

Fig. 25 Chemical potential as function of temperature of present components in the injection gas containing 0.5% H_2S at $P = 230$ bar. The upper dashed curve is chemical potential of liquid water. The lower dashed curve is for chemical potential of water in methane hydrate. The dash-dot curve is the chemical potential of water in an artificial hydrate of structure II formed from a gas composition containing CH_4 , C_2H_6 and C_3H_8 . Solid curves are chemical potential for water in hydrate formed from various CO_2/N_2 ratios. H_2S amount has been added directly as molar ratio and the composition has been normalized. Top curve is for a mole % of CO_2 of 1%. The following curves are for hydrate formed from a mole % of respectively 2, 5, 10, 20, 40, 60, 80% CO_2 from top to bottom

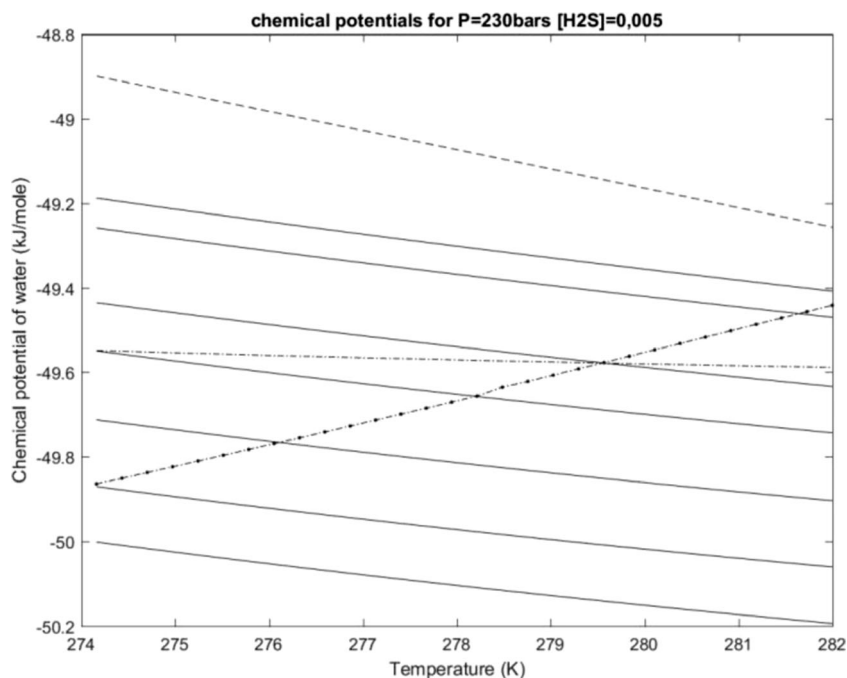
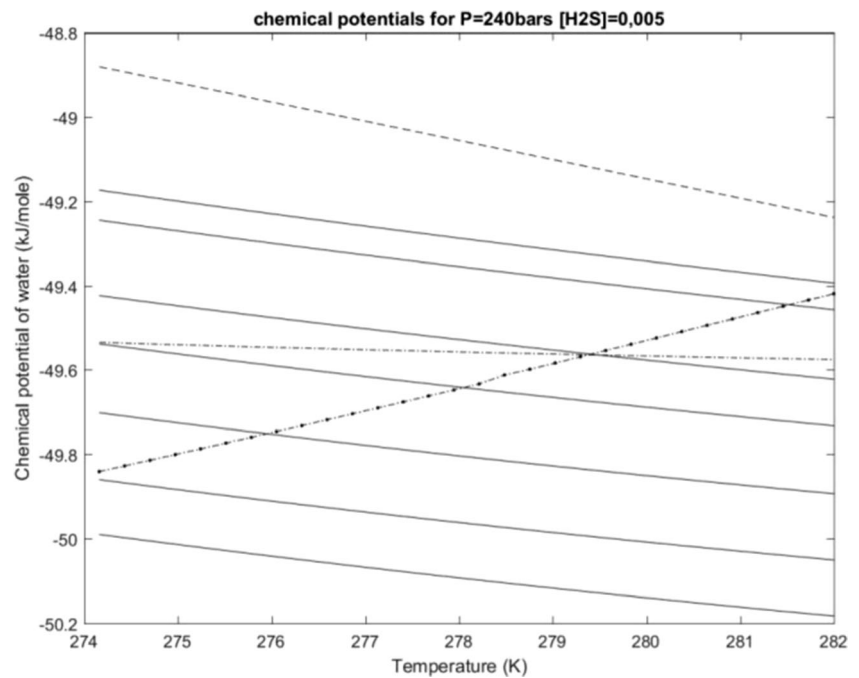


Fig. 26 Chemical potential as function of temperature of present components in the injection gas containing 0.5% H_2S at $P=240$ bar. The upper dashed curve is chemical potential of liquid water. The lower dashed curve is for chemical potential of water in methane hydrate. The dash-dot curve is the chemical potential of water in an artificial hydrate of structure II formed from a gas composition containing CH_4 , C_2H_6 and C_3H_8 . Solid curves are chemical potential for water in hydrate formed from various CO_2/N_2 ratios. H_2S amount has been added directly as molar ratio and the composition has been normalized. Top curve is for a mole % of CO_2 of 1%. The following curves are for hydrate formed from a mole % of respectively 2, 5, 10, 20, 40, 60, 80% CO_2 from top to bottom

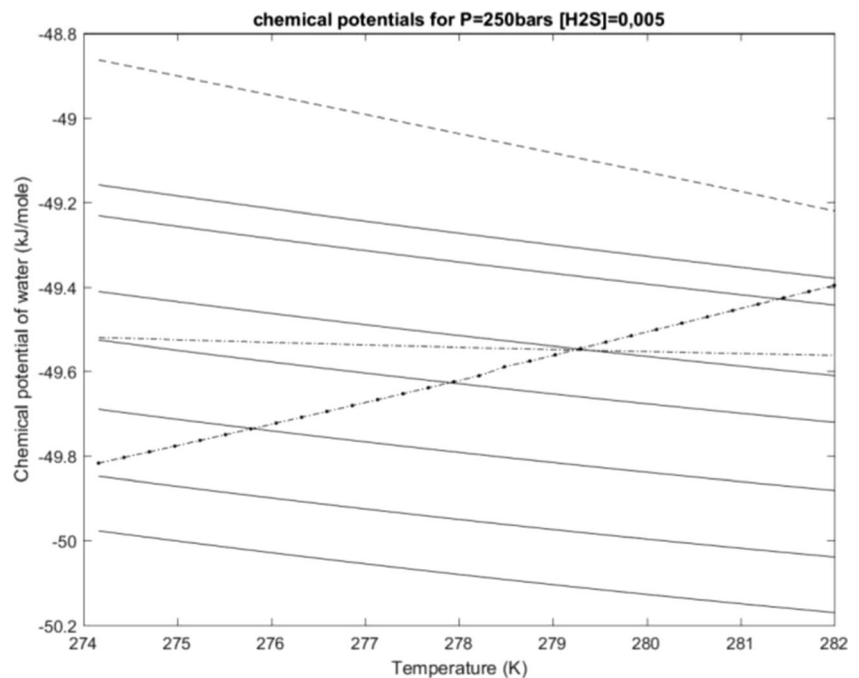


water present in the reservoir, and may never encounter methane hydrates it is supposed to react with. CH_4 substitution by CO_2 in hydrates is limited by the rate of solid diffusion, a slow kinetic phenomenon, which would take place after new hydrates formation, so the CO_2 concentration in injected gas must be calculated to allow CO_2 the time to travel close to the CH_4 hydrates. Therefore, the injected gas composition will be of crucial importance; the amount of N_2 present in the gas

should be judged wisely to optimise hydrate formation without plugging the system.

One of the great advantages of the Natuna gas field lies in its virtual lack of hydrogen sulphide, which acts as inhibitor for chemical transformation of natural gas in addition to being an intensively corrosive agent. This fact allowed us to calculate chemical potential profiles for all the components while ignoring a possible presence of H_2S .

Fig. 27 Chemical potential as function of temperature of present components in the injection gas containing 0.5% H_2S at $P=250$ bar. The upper dashed curve is chemical potential of liquid water. The lower dashed curve is for chemical potential of water in methane hydrate. The dash-dot curve is the chemical potential of water in an artificial hydrate of structure II formed from a gas composition containing CH_4 , C_2H_6 and C_3H_8 . Solid curves are chemical potential for water in hydrate formed from various CO_2/N_2 ratios. H_2S amount has been added directly as molar ratio and the composition has been normalized. Top curve is for a mole % of CO_2 of 1%. The following curves are for hydrate formed from a mole % of respectively 2, 5, 10, 20, 40, 60, 80% CO_2 from top to bottom



Nevertheless, data compiled in the above figures should prove quite relevant for any potential industrial trial considerations.

These figures above clearly show that there exists a range of temperatures and compositions where CO₂ can replace CH₄ in the structure I hydrate. Table 7 below groups these ranges for the pressures concerned.

To summarise, the CO₂ storage coupled with CH₄ recovery from hydrates fields appears to offer a sustainable alternative to combine with gas extraction from high CO₂ concentrated fields. Figures used to illustrate this study are based on seismic data that could be refined further for the purposes of a practical industrial implementation. Nevertheless, the ranges selected are wide enough to include temperatures and variations the most probable in such hydrates fields.

tin formation of CO₂-dominated hydrate and thus enable a rapids mechanism for formation of CO₂ hydrate and release of methane due to heat generated dissociation of *in situ* methane hydrate. A fraction of injected CO₂ will dissolve in the groundwater and adsorb on mineral surfaces. The “enrichment” of CO₂ when it either adsorbs on mineral surfaces or becomes trapped by adsorbed water layers can enhance the overall nucleation rate of the new CO₂ hydrate formation in sediments. But a rigorous estimate of the lowest limit of CO₂ needed in the injection gas will require a detailed modelling for each reservoir in question to make sure that the fast conversion mechanism is retained throughout the reservoir. The extremely slow mechanism of direct solid-state exchange is of not practical importance, but as indicated by Figs. 8 to 25, the concentration of CO₂ in the N₂-dominated mixture needed by the solid-state exchange is higher. In the absence of H₂S in the gas mixture, roughly 5 to 12% CO₂ will be required. These limits will decrease to between 4 to 5% for 0.5% H₂S in the gas mixture and to between 2 to 3% for the case of 1% H₂S. Since the Natuna gas has a very limited presence of higher hydrocarbons, the artificial structure-II gas mixture is not particularly relevant. It is included to provide a qualitative indication of the situation in a reservoir with similar conditions but more thermogenic gas.

7 Conclusion

In this work, we have investigated the Natuna gas as well as two realistic separated streams, a CO₂-rich stream and a methane-rich stream, to determine the maximum water fraction that can be permitted without invoking the risk of hydrate formation. Our estimates suggest that pipeline transport conditions expected for all three streams will fall inside the hydrate formation region if liquid water becomes available either by condensing below the dew-point or adsorbing on rusty pipeline surfaces. The low chemical potential of water adsorbed on hematite (dominating form of rust) will result in

substantially lower tolerance limits for the water content of transported gas. When the water dew-point is used as the criteria, the permitted water mole fraction in gas is roughly eighteen times higher than in the case of using the limit of adsorption on rust.

We have also studied the feasibility of the separated CO₂ for simultaneous safe long terms storage of CO₂ and release of methane from *in situ* hydrates in the North Makassar Basin hydrate field at offshore Indonesia. It was found that the minimum concentration of CO₂ required to create a new hydrate while retaining a fast exchange rate will be reasonably low in case of this deep reservoir. Even CO₂ fractions as low as 2 mol% in CO₂/N₂ gas will allow the new hydrate to form. This is of course a theoretical limit, in practice the injection gas mixture will have to be adjusted depending on hydrate consumption throughout the reservoir. While N₂ will mostly fill the small hydrate cavities, a tiny fraction of it may even enter the large cavities while competing with the far more thermodynamically favoured CO₂. Data available on the Natuna gas indicates that the combined fraction of N₂ and H₂S amounts to 1%. If H₂S accounts for only a half of the admixture, gas able to form a new hydrate is only required to contain as little as 1% of CO₂. Direct solid-state exchange between *in situ* CH₄ hydrate and CO₂ hydrate will be extremely restricted kinetically and of no practical importance. Nevertheless, the minimum level of CO₂ in N₂ required by this mechanism is higher. Roughly 5 to 12% CO₂ will be needed in the absence of H₂S, and 2 to 3% when the mixture contains 1% H₂S.

Compliance with ethical standards

Conflict of interests On behalf of all authors, the corresponding author states that there is no conflict of interests.

Publisher's Note Springer Nature remains neutral with regard to jurisdictional claims in published maps and institutional affiliations.

References

1. Kvamme B et al (2016) Hydrate formation during transport of natural gas containing water and impurities. *J Chem Eng Data* 61(2): 936–949
2. Kvamme B (2016) Thermodynamic Limitations of the CO₂/N₂ Mixture Injected into CH₄ Hydrate in the Ignik Sikumi Field Trial. *J Chem Eng Data* 61(3):1280–1295
3. Fenter DJ, Hadiatno D (1996) Reservoir simulation modeling of natuna gas field for reservoir evaluation and development planning. In: *SPE Asia Pacific Oil and Gas Conference*. Society of Petroleum Engineers
4. Soave G (1972) Equilibrium constants from a modified Redlich-Kwong equation of state. *Chem Eng Sci* 27:1197–1203
5. Kvamme B, Tanaka H (1995) Thermodynamic Stability of Hydrates for Ethane, Ethylene, and Carbon Dioxide. *J Phys Chem* 99(18):7114–7119

6. Kvamme B et al (2014) Consequences of CO₂ solubility for hydrate formation from carbon dioxide containing water and other impurities. *Phys Chem Chem Phys* 16(18):8623–8638
7. Kvamme B et al (2013) Can hydrate form in carbon dioxide from dissolved water? *Phys Chem Chem Phys* 15(6):2063–2074
8. Kvamme B et al (2014) Hydrate phase transition kinetics from Phase Field Theory with implicit hydrodynamics and heat transport. *International Journal of Greenhouse Gas Control* 29:263–278
9. Van der Waals JH, Platteuw JC (1959) *Clathrate solutions*. *Advances in Chemical Physics*, vol 2. Interscience Publishers Inc, New York
10. Sloan ED (2003) Fundamental principles and applications of natural gas hydrates. *Nature* 426(6964):353–363
11. Fan S-S, Guo T-M (1999) Hydrate formation of CO₂-rich binary and quaternary gas mixtures in aqueous sodium chloride solutions. *J Chem Eng Data* 44(4):829–832
12. Maekawa T (2001) Equilibrium conditions for gas hydrates of methane and ethane mixtures in pure water and sodium chloride solution. *Geochem J* 35(1):59–66
13. Jackson BA (2004) Seismic evidence for gas hydrates in the North Makassar Basin, Indonesia. *Pet Geosci* 10(3):227–238